

554 406 468
CM 63-13261
code - 1

TECHNICAL NOTE

D-1616

MEASURED AND CALCULATED SUBSONIC AND TRANSONIC
FLUTTER CHARACTERISTICS OF A 45° SWEPTBACK WING PLANFORM
IN AIR AND IN FREON-12 IN THE LANGLEY
TRANSONIC DYNAMICS TUNNEL

By E. Carson Yates, Jr., Norman S. Land,
and Jerome T. Foughner, Jr.

Langley Research Center
Langley Station, Hampton, Va.

NATIONAL AERONAUTICS AND SPACE ADMINISTRATION
WASHINGTON

March 1963

NATIONAL AERONAUTICS AND SPACE ADMINISTRATION

TECHNICAL NOTE D-1616

MEASURED AND CALCULATED SUBSONIC AND TRANSONIC
FLUTTER CHARACTERISTICS OF A 45° SWEEPBACK WING PLANFORM
IN AIR AND IN FREON-12 IN THE LANGLEY
TRANSONIC DYNAMICS TUNNEL

By E. Carson Yates, Jr., Norman S. Land,
and Jerome T. Foughner, Jr.

SUMMARY

13261

In order to investigate the reliability of flutter data measured in the Langley transonic dynamics tunnel, an experimental and theoretical subsonic and transonic flutter study has been conducted in air and in Freon-12 in this facility. The wing planform employed had an aspect ratio of 4.0, a taper ratio of 0.6, and 45° of quarter-chord sweepback. A sting-mounted full-span model was tested in addition to three sizes of wall-mounted semispan models. A wide range of mass ratio was covered by the tests in air and by flutter calculations made by the modified strip-analysis method of NACA Research Memorandum L57L10. A limited amount of data was obtained in Freon-12.

Results of the tests in air and in Freon-12 are in good agreement with the flutter calculations at all Mach numbers. The test data compare favorably with previously published transonic flutter data for the same wing planform. The results indicate that flutter characteristics obtained in Freon-12 may be interpreted directly as equivalent flutter data in air at the same mass ratio and Mach number.

INTRODUCTION

In order to investigate the reliability of subsonic and transonic flutter data obtained in the Langley transonic dynamics tunnel, it is desirable to compare flutter data obtained in this facility with flutter data from another facility and with the results of proven theoretical methods. This report shows such comparisons for a moderately swept, moderately tapered, wing planform that has been the subject of previous extensive experimental and theoretical flutter investigations. Since the Langley transonic dynamics tunnel is designed to use either air or

Freon-12 as a testing medium, flutter results were obtained in both media. At a given temperature and pressure, Freon-12 is about four times as dense as air and has a speed of sound 55 percent lower than that for air. For dynamic testing, these properties make Freon-12 an attractive alternate to air for the following reasons: (1) A given mass-density ratio may be attained with heavier models, (2) data readout and test observation are simplified because of slower time scale, and (3) at a given Mach number, much greater fluid density may be used with a given amount of drive-motor power.

The possibilities of using Freon-12 as a fluid for aerodynamic testing have been examined in reference 1 where the thermodynamic properties were investigated. Reference 2 shows comparisons of steady-flow aerodynamic coefficients measured in Freon-12 and in air for both swept and unswept wings. Freon-12 was used as a medium for dynamic testing in reference 3 where an experimental and analytical investigation of the flutter of sweptback cantilever wings is reported.

The models tested in the present investigation had a panel aspect ratio of 1.6525, a panel taper ratio of 0.6576, a quarter-chord sweep-back angle of 45° , and NACA 65A004 airfoil sections in the streamwise direction. Reference 4 presents transonic flutter characteristics of this wing planform as obtained in the Langley transonic blowdown tunnel. References 5 to 7 present subsonic, transonic, and supersonic flutter characteristics for this wing planform as calculated by the modified strip-analysis method of reference 5, and good agreement is shown with the experimental data of reference 4.

Results of the present flutter tests in air at Mach numbers from 0.34 to 1.14 are also compared with corresponding calculations made by the method of reference 5 and with the experimental data of reference 4. A limited amount of flutter data measured in Freon-12 at Mach numbers from 0.73 to 1.00 is compared with similar calculations.

A comparison, based on a limited amount of data, was obtained in air between flutter characteristics of wall-mounted semispan models and sting-mounted full-span models at low Mach numbers.

SYMBOLS

- $a_{c,n}$ nondimensional distance from midchord to local aerodynamic center (for steady flow) measured perpendicular to elastic axis, positive rearward, fraction of semichord measured perpendicular to elastic axis (called ac_n in refs. 5 to 7)
- b_s streamwise semichord measured at wing root

b_t	streamwise semichord measured at wing tip
$c_{l_{\alpha,n}}$	local lift-curve slope for a section normal to elastic axis in steady flow
c_n	section normal-force coefficient
$\Delta c_n = c_{n,F} - c_{n,A}$	
EI	bending stiffness
GJ	torsional stiffness
$f_{h,i}$	natural frequency of wing in i th coupled bending mode
$f_{t,j}$	natural frequency of wing in j th coupled torsion mode
f_α	natural frequency of wing in first uncoupled torsion mode
k_{nr}	reduced frequency based on velocity component normal to elastic axis and on semichord normal to elastic axis at 0.75 spanwise station
M	Mach number
\bar{m}	measured wing panel mass
q	dynamic pressure
s	wing panel span
V	stream velocity
v	volume of a conical frustum having streamwise root chord as lower base diameter, streamwise tip chord as upper base diameter, and panel span as height
η	nondimensional coordinate along elastic axis measured from wing root, fraction of elastic axis length
Λ_{ea}	sweep angle of wing elastic axis, positive for sweepback
$\bar{\mu}$	mass ratio, $\frac{\bar{m}}{\rho v}$
ρ	test-medium mass density

ω	flutter frequency
ω_α	natural circular frequency of wing in first uncoupled torsion mode, $2\pi f_\alpha$

Subscripts:

A	air
F	Freon-12
calc	calculated
meas	measured

MODELS

Model Geometry

The models tested had a panel aspect ratio of 1.6525, a panel taper ratio of 0.6576, a quarter-chord sweepback angle of 45° , and NACA 65A004 airfoil sections in the streamwise direction. These values of panel aspect ratio and panel taper ratio coincide with those of reference 4 and correspond to a full-span wing of aspect ratio 4.0 and taper ratio 0.6 which is mounted on a fuselage that covers 21.90 percent of the wing span. Figure 1 gives the wing panel dimensions of the sting-mounted full-span model and of the three sizes of wall-mounted semispan models employed in this investigation. The full-span model was mounted at 0° incidence on an 8-inch-diameter ogive-cylinder fuselage. The ratio of fuselage diameter to wing span for this model was 0.22, the same as for the models of reference 4. Figure 2 shows the 3.00-foot full-span (1.167-foot panel span) model mounted on the fuselage. It should be noted particularly that the present full-span model had a fuselage of limited nose length, whereas the models of reference 4 were mounted on an elongated sting fuselage that extended into the subsonic flow region of the tunnel entrance cone.

Model Construction

The models were constructed of laminated mahogany and hence were essentially homogeneous like those of reference 4. Figure 2 shows a photograph of the solid full-span model and figure 3 shows a typical solid semispan model.

In order to obtain flutter throughout the tunnel Mach number and density ranges, it was necessary to reduce the stiffness of some of the models. Six of the 2.500-foot wall-mounted semispan models were reduced in stiffness by drilling holes through the wing normal to the chord plane, as described in reference 8. A rigid foam plastic was used as a filler to maintain aerodynamic continuity without appreciably altering the stiffness of the perforated wing. A model in which the stiffness was reduced in this manner is referred to herein as a weakened model. (See figs. 4 and 5.)

Model Identification

The models tested are divided into sting-mounted full-span model and wall-mounted semispan models. Only a single full-span model (fig. 1) was tested. The wall-mounted semispan models are subdivided into solid models of 1.250-foot, 2.500-foot, and 3.750-foot panel span; and weakened models of 2.500-foot panel span. In only two cases, the 2.500-foot solid and weakened semispan series, were more than one model tested. Individual models of these two series are designated in the tables by numbers. Due to close similarity of the model properties in these series, no distinction is made between individual models in the figures.

Model Physical Properties

Some model physical properties are indicated in table I which presents the measured frequencies of the first four vibrational modes for each model together with the wing panel mass. A description of the method of frequency measurement is given in reference 9. Representative node-line patterns for all the semispan models and for the full-span model are shown in figures 6 and 7, respectively.

The distributions of the bending and torsional stiffnesses, EI and GJ , for all of the models were measured by the method described in reference 8. Figures 8 to 10 show the measured distributions of EI and GJ for representative models.

TUNNEL AND APPARATUS

General Description of Tunnel

The Langley transonic dynamics tunnel, shown in figure 11, is a return-flow, variable-pressure, slotted-throat tunnel having a test section 16 feet square (with cropped corners). It is capable of operation at stagnation pressures from near vacuum to slightly above one

atmosphere and at Mach numbers from 0 to 1.2. The tunnel is designed to use either air or Freon-12 as the test medium. Curves showing the tunnel operating ranges are presented in figure 12 for air and in figure 13 for Freon-12. This tunnel is particularly suited to flutter research and general dynamic testing because Mach number and dynamic pressure can be varied independently. In addition, the tunnel is equipped with a quick-opening bypass valve (fig. 11) which can be opened when flutter occurs in order to reduce rapidly the dynamic pressure in the test section.

Model Mounts

The semispan models were mounted cantilevered from the tunnel test-section wall with no provision made to avoid the wall boundary layer. Figure 5 is a photograph of a weakened semispan model mounted in the tunnel in this manner.

The full-span model was sting-mounted and located on the tunnel center line. The fundamental bending frequency of the sting support with model installed was 5.6 cycles per second as compared with the lowest model frequency (first bending) of 30.6 cycles per second.

Instrumentation

Each model was instrumented with strain gages externally mounted near the wing root and oriented so as to distinguish between wing bending and torsional deflections. The strain-gage signals were recorded on a multichannel oscillograph and displayed on a cathode-ray oscilloscope to aid the model observer in determining the approach of flutter. Visual records of wing deflections were obtained from 16-mm motion pictures taken at 128 frames per second. During tests of the sting-mounted full-span model, sting displacements were indicated by an accelerometer attached to the fuselage.

Tunnel stagnation temperature, stagnation pressure, and static pressure were measured and automatically tabulated for each test point. For tests in Freon-12, the Freon purity was measured by a purity meter based on the variation of thermal conductivity with the Freon content of the testing medium. For the present tests, Freon-12 purity was always above 91 percent by volume (or 98 percent by weight).

FLUTTER TEST PROCEDURE

The tests were conducted with the model set at a condition of zero total lift. This setting was attained by monitoring the oscillograph traces of the bending-moment gages while the tunnel was at a low dynamic pressure and adjusting the model angle of attack so that the root bending moment was zero.

The initial step in obtaining a flutter point was to estimate the model flutter boundary by using the data of reference 4 as a guide. A tunnel stagnation pressure was then selected to intersect this estimated boundary near a desired Mach number. Model data and tunnel conditions were recorded at intervals as the dynamic pressure was slowly increased. After a flutter condition was established, an attempt was made to save the model by reducing the dynamic pressure as quickly as possible by opening the tunnel bypass valve and by reducing the tunnel fan speed. These attempts were successful to the extent that only seven models were damaged in obtaining 25 flutter points.

The accuracy of determining the dynamic pressure at flutter in these tests is considered to be ± 2 pounds per square foot.

FLUTTER CALCULATIONS

All flutter calculations of this investigation were made by the modified-strip-analysis method of references 5 and 6. This method employs spanwise distributions of lift and pitching moment derived from distributions of aerodynamic parameters associated with the undeformed wing in steady flow.

In all the present calculations, three calculated uncoupled vibrational modes (first and second bending and first torsion) were employed. The modal frequencies (table I) for each model, however, were obtained from measured coupled-mode frequencies. As in the procedure of reference 4, measured frequencies for coupled bending modes were used directly as uncoupled bending-mode frequencies. Measured coupled torsion-mode frequencies were "uncoupled" by means of the relation used in reference 4. The node-line positions for the present models (figs. 6 and 7) indicate that the natural modes for these models are not highly coupled; therefore, this procedure should give reasonably accurate estimates of the uncoupled-mode frequencies.

As mentioned previously, the unweakened (solid) models were of essentially homogeneous construction. Although the weakened models were

not homogeneous, the foam-plastic-filled holes in them were spaced fairly uniformly over the wing surface. Accordingly, all models were treated as homogeneous in the flutter calculations.

In all calculations the models were considered to be cantilevered from the root. This condition should be correct for the wall-mounted models, but some root motion did occur for the sting-mounted model.

Calculations Corresponding to Tests in Air

For each flutter point measured in air at Mach number less than 1.0, the corresponding flutter calculation was based on the mass and stiffness properties of the model tested and on the experimental values of Mach number and flow density. In these calculations the required spanwise distributions of steady-flow section lift-curve slope and local aerodynamic center were calculated from subsonic lifting-surface theory, essentially that of reference 10. In addition to the subsonic calculations, a calculation was made for model 3 of the 2.500-foot weakened

series at a Mach number of $\frac{2}{\sqrt{3}} = 1.15470$ and at the density associated with the measured flutter point at $M = 1.141$. Aerodynamic parameters for this calculation were obtained from the supersonic lifting-surface theory of reference 11.

In addition to these theoretical aerodynamic parameters, some experimentally determined distributions of section lift-curve slope and local aerodynamic center were used in flutter calculations at Mach numbers from 0.6 to 1.2. These measured aerodynamic parameters have been used previously in flutter calculations for other wings of the present planform and are shown in figures 1 and 2 of reference 6. For the present flutter calculations employing measured aerodynamic parameters, the densities used were those associated with the experimental flutter point at the nearest adjacent Mach number.

Finally, aerodynamic parameters calculated from the subsonic and supersonic lifting-surface theories were employed in flutter calculations for model 3 of the 2.500-foot weakened series at Mach numbers of 0, 0.90, and $\frac{2}{\sqrt{3}}$ and at several values of density in order to show the variation of flutter-speed coefficient with density (or mass ratio).

Calculations Corresponding to Tests in Freon-12

Flutter calculations corresponding to flutter points measured in Freon-12 followed the general procedure outlined previously, except that

the aerodynamic parameters were modified to account for the difference between Freon-12 and air. Reference 2 showed that at a given subsonic or transonic Mach number, steady-flow aerodynamic coefficients measured in Freon-12 can be significantly higher than those measured in air, the differences rising to about 10 percent at Mach numbers near 1.0. In addition, reference 2 showed that pitching moment and normal force were affected in the same way and to about the same extent. The differences between air and Freon-12 thus manifested themselves as differences in load levels but did not change loading centers. Accordingly, in the flutter calculations these differences between air and Freon-12 were accounted for by increasing the section lift-curve slope for the Freon-12 calculations by a fraction which varied with Mach number as shown for two-dimensional wings in figure 16 of reference 2. In accordance with the modified-strip-analysis procedure as given in reference 5, this lift-curve-slope correction was determined by the Mach number component normal to the leading edge. No alterations were made in the aerodynamic-center locations. Thus, since lift and normal force approach each other at vanishingly small angles of attack, the corrections of the aerodynamic parameters used in the flutter calculations for Freon-12 were made as follows:

$$(c_{l_{\alpha,n}})_F = \frac{(c_{l_{\alpha,n}})_A}{1 - \frac{\Delta c_n}{c_{n,F}}} \quad (1)$$

and

$$(a_{c,n})_F = (a_{c,n})_A \quad (2)$$

where $\frac{\Delta c_n}{c_{n,F}} = \frac{c_{n,F} - c_{n,A}}{c_{n,F}}$ is given as a function of Mach number in figure 14 (from fig. 16 of ref. 2).

RESULTS AND DISCUSSION

The flutter data measured in air and in Freon-12 for all models are summarized in tables II and III and are shown in relation to the tunnel operating boundaries in figures 12 and 13. It is evident that a number of the flutter points in both air and Freon-12 were reached at dynamic pressures near the maximum obtainable.

The ranges of mass ratio and Mach number covered in the present tests both in air and in Freon-12 are shown in figure 15. Most of the

points shown lie in the mass-ratio range $8.4 < \bar{\mu} < 69.7$ and hence would be pertinent, for example, to current fighter-type airplanes at low to moderate altitude. On the other hand, the comparatively high mass ratios shown for the 2.500-foot weakened models in air would be appropriate for modern airplanes at very high altitude.

Figure 16 shows the measured flutter-speed coefficients and flutter-frequency ratios which correspond to the test conditions of figure 15. The flutter speeds and frequencies for each series of models in either air or Freon-12 appear to be consistent among themselves. However, large differences exist between results for the weakened models in air and in Freon-12 and between results for the weakened and solid models in Freon-12. The sequel will show that these differences are caused primarily by differences in mass ratio (fig. 15).

Air

The closeness of the three measured flutter points at Mach numbers 0.95 to 0.96 for model 3 of the 2.500-foot weakened semispan series (fig. 16) indicates excellent repeatability of the present flutter tests in the transonic dynamics tunnel. Furthermore, the flutter points for the 2.500-foot solid and weakened wall-mounted models are close together. Figure 16 shows that the single flutter point for the 3.750-foot solid wall-mounted model is in close proximity to the data for the 2.500-foot solid models. No flutter was obtained, however, on the 1.250-foot solid wall-mounted model. The no-flutter points shown for this model represent the maximum tunnel dynamic pressure attainable in air (fig. 12).

Tests of the 2.500-foot weakened models indicate an upturn of the flutter-speed-coefficient curve as Mach number decreases toward 0.3. This upturn is attributed to the accompanying decrease in mass ratio (fig. 15). References 7 and 12 have shown that for a given Mach number, flutter-speed coefficient typically increases as mass ratio decreases.

Figure 16 shows that the subsonic flutter speeds recorded for the sting-mounted full-span model compare very favorably with the data for the wall-mounted semispan models. Although the sting-mounted model experienced some bounce at the sting first bending frequency (5.6 cycles per second), the component of wing-root flutter motion at the flutter frequency (65 cycles per second) was of the order of only 0.0025 inch.

Flutter speeds and frequencies for the wall-mounted models calculated by the method of reference 5 and employing both theoretical and measured steady-flow aerodynamic parameters are in good agreement with the experimental flutter data throughout the Mach number range (fig. 17). In all cases the calculated flutter-speed coefficients are within about

6 percent of the measured values. In reference 6, flutter calculations made by the same procedure employed in the present report showed good agreement with the flutter data of reference 4 for the same wing planform. For the sting-mounted model the calculated flutter-speed coefficient is slightly higher than the measured points. The fact that root freedom was not taken into account in the calculations is believed to effect most of this difference.

Freon-12

Figure 18 shows calculated flutter speeds for Freon-12 to be in satisfactory agreement with measured values, although there are significant differences between the levels of flutter-speed coefficient for weakened and solid models. It should be pointed out that the experimentally determined aerodynamic coefficients used in some of the flutter calculations were measured on 6-percent-thick wings rather than on 4-percent-thick wings which were flutter tested. (See also ref. 6.) If distributions of section aerodynamic coefficients were available for 4-percent-thick wings, the calculated flutter speeds in Freon-12 and in air would be expected to be slightly higher at Mach numbers near 1.0 and in slightly better agreement with experiment. Reference 6 indicates that use of measured aerodynamic parameters for a 4-percent-thick wing might be expected to result in a somewhat shallower dip in the calculated flutter speeds for Mach numbers near 1.0.

The reason for the discrepancy between calculated values of flutter speed and frequency and the single measured flutter point at Mach number 1.0 is not known. It is thought, however, that the low level of measured flutter speed and frequency at this Mach number may be associated with disturbances reflected from the tunnel walls.

As mentioned previously, the flutter calculations shown in figure 18 included a small modification to the section lift-curve slopes in order to account for the difference between aerodynamic-load intensities in Freon-12 and in air. Supplementary calculations have shown that neglecting this correction would result in calculated flutter speeds slightly higher (4 percent or less) than those shown in figure 18. Neglecting this correction would improve slightly the comparison between calculated and measured flutter speeds for the solid wings (fig. 18) but would have a slightly adverse effect on the comparisons for the weakened wings. Therefore, the present flutter points do not give a clear-cut indication of the appropriateness of this correction. In any event, for subsonic and transonic Mach numbers the correction appears to have only a small effect on the present flutter speeds. It appears, therefore, that the correction may be reasonably neglected in the interpretation of Freon-12 flutter data in terms of equivalent air data for planforms similar to the present one. That is, flutter data obtained in Freon-12

may be interpreted directly as flutter data in air at the same mass ratio and Mach number. This direct interpretation would result in a slightly conservative estimate of the flutter boundary. However, for purposes of estimating the flutter boundary for a model that is to be tested in Freon, the correction probably should be used.

It should be emphasized that these statements are pertinent only to a single phenomenon (flutter), and the present investigation is limited to a single planform. For wings with planforms significantly different from the present, for higher Mach numbers, for other aerodynamic shapes, or for other phenomena, some correction of Freon data may be required.

Effect of Mass Ratio

Figure 16 shows that at a given Mach number, significant differences exist in the levels of transonic flutter-speed coefficients between tests in air and in Freon-12 and between tests of solid and weakened models in Freon-12. The good agreement between calculated and measured flutter speeds (figs. 17(a) and 18(a)), however, indicates that these sizable differences are caused predominantly by differences in mass ratio. In spite of the large range of mass ratio covered by the present tests, flutter characteristics measured both in air and Freon-12 are satisfactorily correlated by the modified strip analysis (fig. 19).

The effects of mass-ratio variation on subsonic and supersonic flutter characteristics for a variety of wing planforms have been studied theoretically in references 7 and 12. Similar effects of mass ratio (or density) are shown for the present wings in figures 20 and 21. It should be noted specifically in figure 20 that flutter-speed coefficient becomes very sensitive to density changes when the density level is low. In other words, at low densities small discrepancies in density can lead to large deviations in flutter-speed coefficient. Therefore, there may be reason to doubt that the present close agreement between measured and calculated flutter speeds could be generally obtained at the low density levels associated with some of the tests in air. However, figure 21 shows that the flutter reduced frequency for a given wing generally decreases as density decreases. As indicated in reference 5 the flutter-analysis method employed herein would be expected to become more accurate as reduced frequency decreases.

Comparison With Data From the Langley Transonic Blowdown Tunnel

In figure 22 all the flutter speeds and frequencies measured in the Langley transonic dynamics tunnel are compared with the flutter data of reference 4 which were obtained in the Langley transonic blowdown tunnel. Although the data from the two facilities overlap only in the transonic

range, the two sets of flutter speeds and frequencies appear to be generally consistent with each other. At Mach numbers below 1.0, the mass ratios associated with the data of reference 4 lie between those for the present tests of the 2.500-foot weakened models in air and in Freon-12 (fig. 22). Consequently most of the flutter-speed points from reference 4 lie near or between the curves for the weakened models in air and in Freon-12. At Mach numbers above 1.0, mass ratios for the present tests in air in the transonic dynamics tunnel are much higher than those for the tests in the transonic blowdown tunnel; therefore, the present flutter-speed coefficients are lower than those from reference 4.

The consistency of the present data with those of reference 4 (fig. 22) is supported by calculations by the method of reference 5. In particular, these calculations (fig. 20) indicate that for a given Mach number, lower flutter-speed coefficients would be associated with higher mass-ratio values. (See also, for example, figs. 48 and 59 of ref. 7.) The calculations also indicate that flutter-speed coefficients are more sensitive to mass-ratio differences at supersonic Mach numbers than in the subsonic range.

CONCLUSIONS

An experimental subsonic and transonic flutter investigation of a 45° sweptback wing planform has been conducted in air in the Langley transonic dynamics tunnel. A limited amount of data was also obtained in Freon-12. Comparisons of the results with corresponding theoretical analyses and with experimental results from another facility indicate the following conclusions:

1. Flutter data measured in the Langley transonic dynamics tunnel appear to be generally consistent with flutter data obtained in the Langley transonic blowdown tunnel.
2. Subsonic and transonic flutter characteristics obtained in Freon-12 may reasonably be interpreted directly as equivalent flutter data in air at the same mass ratio and Mach number. This direct interpretation, however, would result in a slightly conservative estimate of the flutter boundary.
3. At all Mach numbers, flutter calculations made by a modified-strip-analysis method are in good agreement with the measured flutter data in both air and Freon-12.

4. The differences between subsonic flutter characteristics measured with 2.500-foot and 3.750-foot wall-mounted semispan models are insignificant. Subsonic flutter characteristics for the sting-mounted full-span model compare favorably with the flutter data for the wall-mounted semispan models.

5. The wide range of mass ratio covered in this investigation caused sizable differences in flutter-speed coefficients (for a given Mach number) both experimentally and theoretically.

Langley Research Center,
National Aeronautics and Space Administration,
Langley Air Force Base, Va., March 6, 1962.

REFERENCES

1. Huber, Paul W.: Use of Freon-12 As a Fluid for Aerodynamic Testing. NACA TN 1024, 1946.
2. Von Doenhoff, Albert E., Braslow, Albert L., and Schwartzberg, Milton A.: Studies of the Use of Freon-12 as a Wind-Tunnel Testing Medium. NACA TN 3000, 1953.
3. Barmby, J. G., Cunningham, H. J., and Garrick, I. E.: Study of Effects of Sweep on the Flutter of Cantilever Wings. NACA Rep. 1014, 1951. (Supersedes NACA TN 2121.)
4. Jones, George W., Jr., and Unangst, John R.: Investigation To Determine Effects of Center-of-Gravity Location on Transonic Flutter Characteristics of a 45° Sweptback Wing. NACA RM L55K30, 1956.
5. Yates, E. Carson, Jr.: Calculation of Flutter Characteristics for Finite-Span Swept or Unswept Wings at Subsonic and Supersonic Speeds by a Modified Strip Analysis. NACA RM L57L10, 1958.
6. Yates, E. Carson, Jr.: Use of Experimental Steady-Flow Aerodynamic Parameters in the Calculation of Flutter Characteristics for Finite-Span Swept or Unswept Wings at Subsonic, Transonic, and Supersonic Speeds. NASA TM X-183, 1960.
7. Yates, E. Carson, Jr.: Some Effects of Variations in Density and Aerodynamic Parameters on the Calculated Flutter Characteristics of Finite-Span Swept and Unswept Wings at Subsonic and Supersonic Speeds. NASA TM X-182, 1960.
8. Land, Norman S., and Abbott, Frank T., Jr.: Method of Controlling Stiffness Properties of a Solid-Construction Model Wing. NACA TN 3423, 1955.
9. Jones, George W., Jr., and DuBose, Hugh C.: Investigation of Wing Flutter at Transonic Speeds for Six Systematically Varied Wing Plan Forms. NACA RM L53G10a, 1953.
10. Falkner, V. M.: The Calculation of Aerodynamic Loading on Surfaces of Any Shape. R. & M. No. 1910, British A.R.C., Aug. 1943.
11. Cohen, Doris: Formulas for the Supersonic Loading, Lift, and Drag of Flat Swept-Back Wings With Leading Edges Behind the Mach Lines. NACA Rep. 1050, 1951.

12. Yates, E. Carson, Jr.: Subsonic and Supersonic Flutter Analysis of a Highly Tapered Swept-Wing Planform, Including Effects of Density Variation and Finite Wing Thickness, and Comparison With Experiments. NASA TM X-764, 1963.

TABLE I
MEASURED MODAL FREQUENCIES AND PANEL MASS

Model description				Frequency, cps					Panel mass, slugs
Panel span, ft	Mounting	Structure	Model	f _{h,1}	f _{h,2}	f _{t,1}	f _{t,2}	f _α	m̄
1.250	Wall	Solid	1	30.40	146.00	99.10	243.00	98.77	0.02298
2.500	Wall	Solid	1	14.60	67.30	47.70	117.00	47.54	.14347
			2	14.10	69.30	50.70	127.10	50.68	.14658
2.500	Wall	Weakened	1	9.70	47.00	35.00	89.50	34.89	.13758
			2	10.10	49.00	33.80	89.00	33.69	.13665
			3	9.60	50.70	38.10	98.50	38.09	.12764
			4	9.70	51.00	38.00	98.50	37.88	.12764
			5	9.80	54.20	39.20	96.50	39.07	.12143
			6	10.00	51.20	38.90	98.50	38.77	.12826
3.750	Wall	Solid	1	8.60	40.90	32.30	79.70	32.29	.51304
1.167	Sting	Solid	Left	30.60	143.00	99.00	268.00	98.67	*.01899
			Right	31.20	143.00	97.00	251.00	96.97	*.01899

* Calculated panel mass.

TABLE II

FLUTTER DATA MEASURED IN AIR

Model description				M	ρ , slugs/cu ft	$\bar{\mu}$	ω , radians/sec	ω , radians/sec	V , ft/sec	q , lb/sq ft	$\frac{V}{b_g a_c \sqrt{\mu}}$
Panel span, ft	Mounting	Structure	Model								
1.250	Wall	Solid	*1	0.480	0.00208	19.250	620.6	620.6	540.83	306.8	0.4333
			*1	.470	.00209	19.158	620.6	620.6	530.05	295.4	.4256
	Wall	Solid	1	.451	.00216	14.455	298.7	298.7	507.8	279.6	.4879
2.500	Wall	Solid	1	.463	.00209	14.939	298.7	298.7	522.9	288.0	.4942
			1	.850	.000155	193.150	219.2	219.2	977.8	64.2	.3502
	Wall	Weakened	1	.870	.000155	193.150	219.2	219.2	933.5	66.2	.3343
3.750	Wall	Solid	2	.834	.000206	144.350	211.7	211.7	901.1	82.7	.3865
			3	.901	.000193	143.920	239.3	239.3	973.4	89.3	.3700
			3	.678	.000404	68.753	239.3	239.3	759.1	115.7	.4174
			3	.499	.000830	33.465	239.3	239.3	565.8	133.1	.4459
			3	.954	.000123	225.820	239.3	239.3	1,008.4	60.6	.3059
			3	.960	.000123	225.820	239.3	239.3	1,013.8	61.3	.3076
			3	.957	.000123	225.820	239.3	239.3	1,020.2	61.7	.3095
			3	1.072	.000107	259.590	239.3	239.3	1,131.0	66.1	.3201
			3	1.141	.000152	182.740	239.3	239.3	1,195.3	105.3	.4031
			4	.338	.00221	12.568	238.0	238.0	383.4	163.9	.4958
	Wall	Solid	1	.496	.00194	17.055	202.9	202.9	569.0	316.0	.4938
	Sting	Solid	Right panel	.466	.00199	20.291	608.97	608.97	529.0	282.5	.4500
1.167			Right panel	.458	.00202	19.989	608.97	608.97	524.5	279.6	.4496

*No flutter.

TABLE III
FLUTTER DATA MEASURED IN FREON-12

Model description			M	ρ , slugs/cu ft	$\bar{\mu}$	ω_0 , radians/sec	ω , radians/sec	V, ft/sec	q , lb/sq ft	$\frac{V}{b_s \omega_0 \sqrt{\bar{\mu}}}$
Panel span, ft	Mounting	Structure								
2.500	Wall	Solid	2	0.00267	11.947	318.4	165.2	516.5	349.4	0.5121
			2	.00312	10.224	318.4	169.6	482.8	364.3	.5175
			2	.00343	9.300	318.4	172.1	464.1	367.5	.5214
			2	.00377	8.461	318.4	169.6	441.1	361.7	.5196
2.500	Wall	Weakened	5	.000787	33.576	245.5	101.7	507.3	100.8	.3891
			5	.00107	24.696	245.5	113.0	467.4	115.9	.4180
			6	.00228	12.242	243.6	136.9	372.0	156.7	.4762
			6	.00230	12.135	243.6	129.4	366.8	154.4	.4716

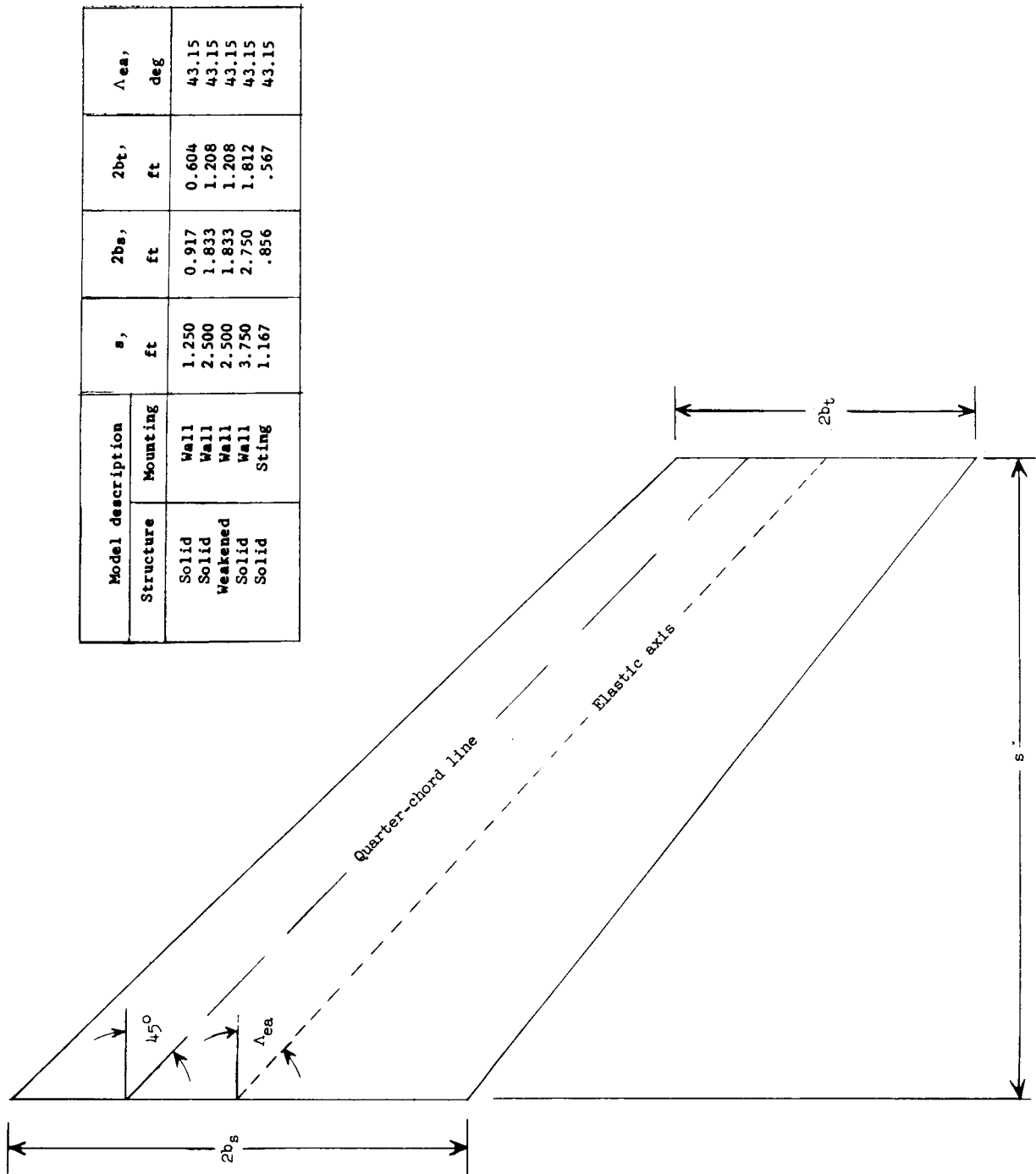


Figure 1.- Wing panel dimensions.

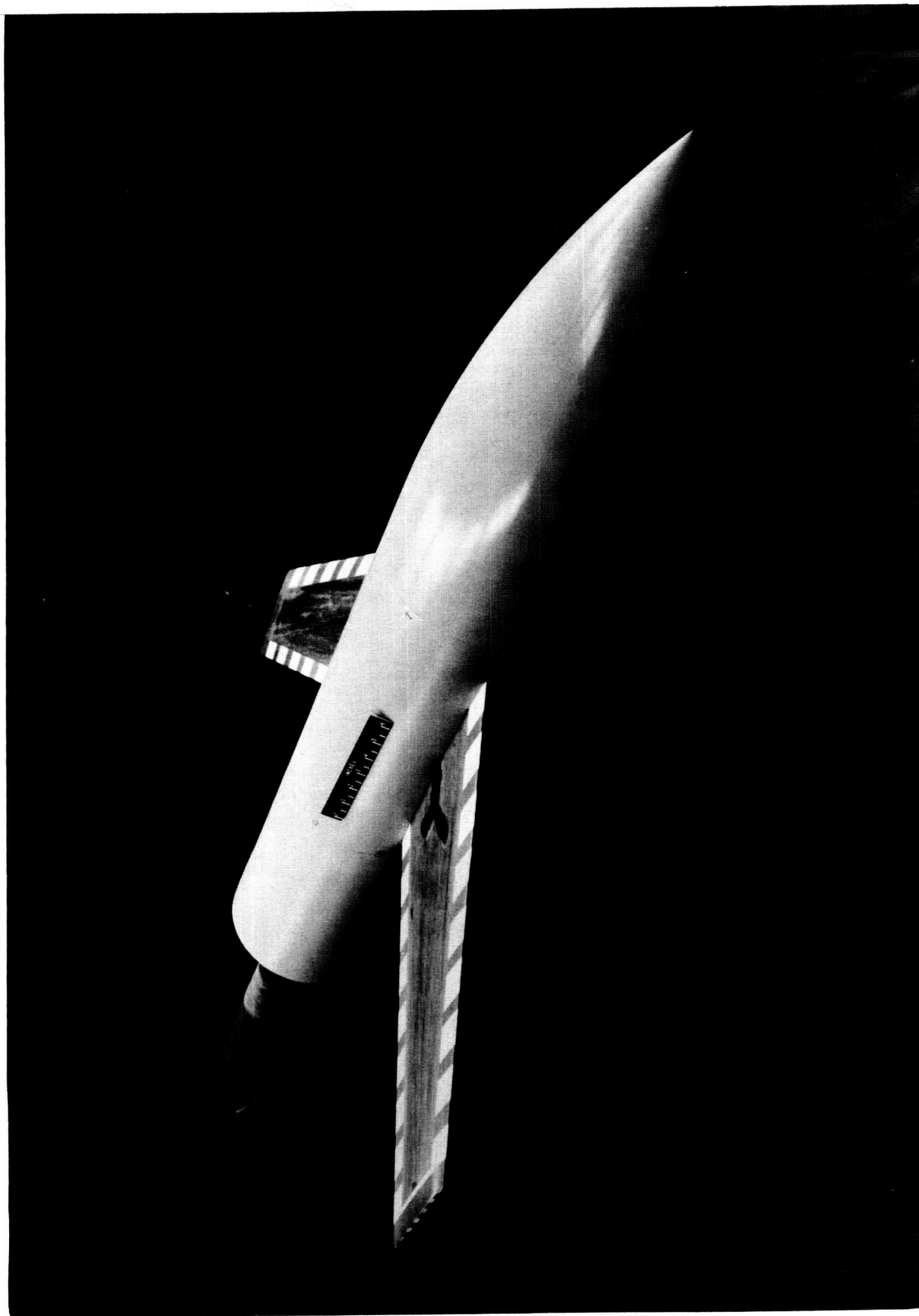


Figure 2.- Full-span model on fuselage. L-60-2610

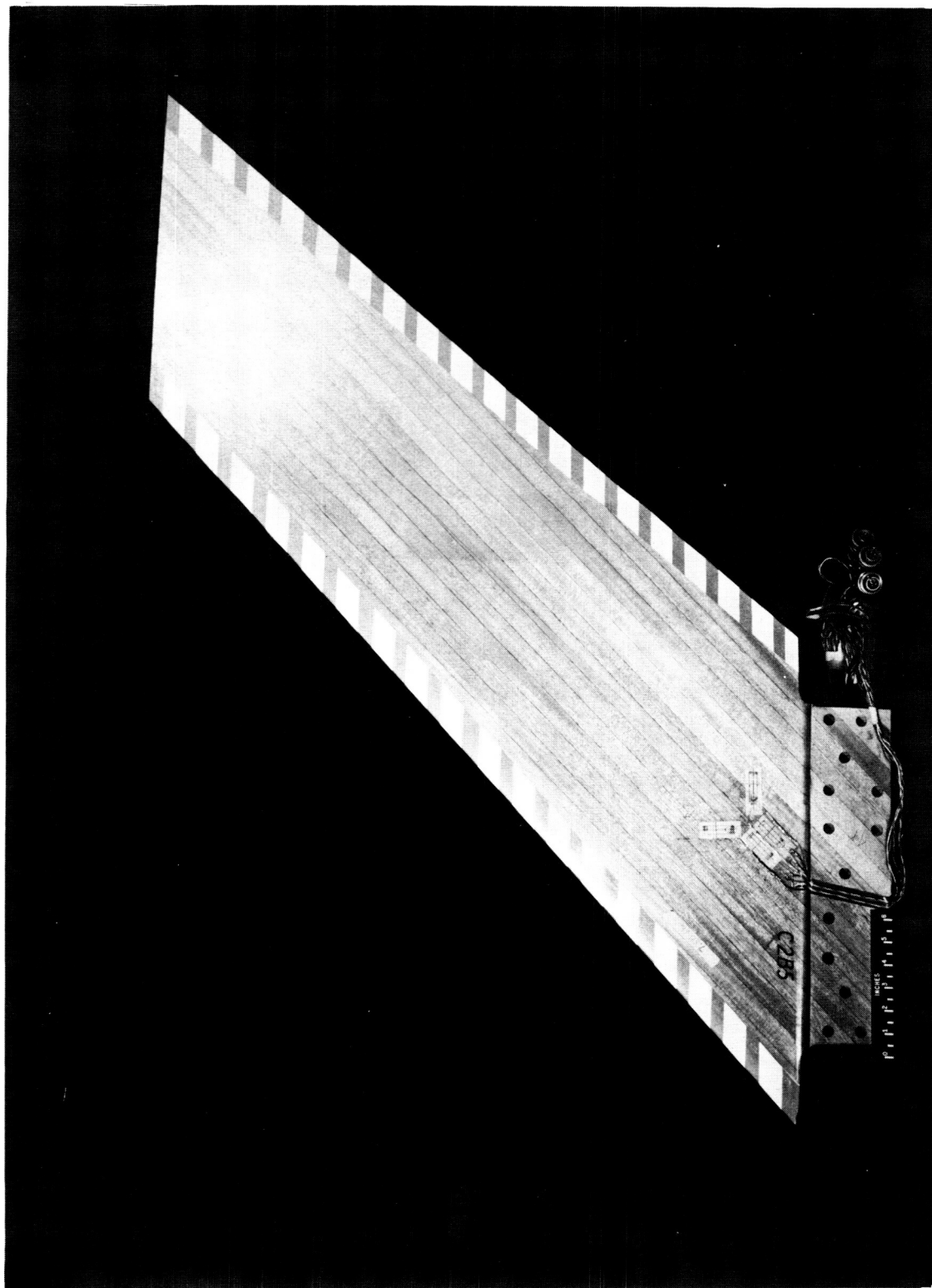


Figure 3.- Typical solid semispan model.

L-60-2607

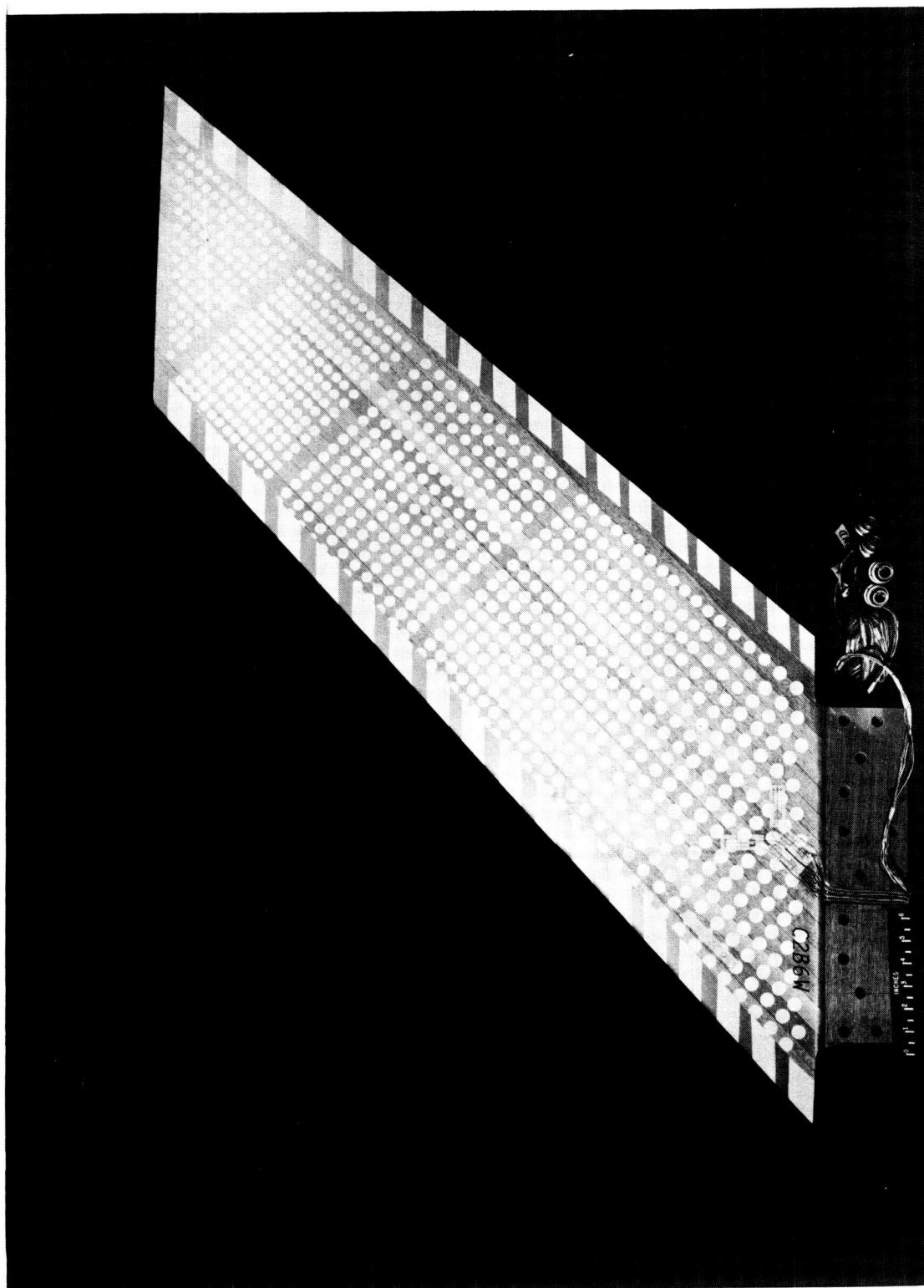


Figure 4.- Weakened semispan model. L-60-2609

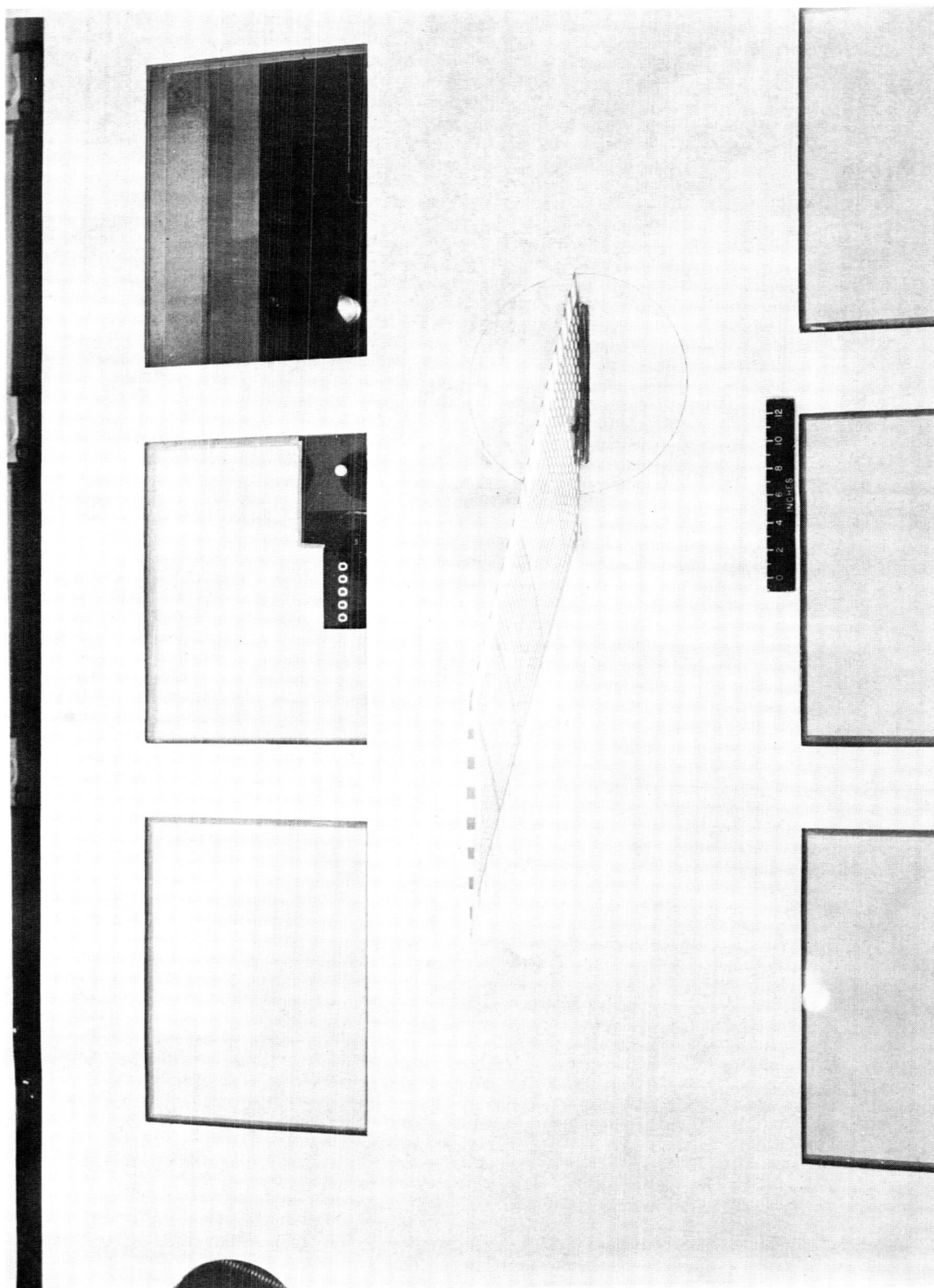


Figure 5.- Weakened model mounted in tunnel.

L-60-964

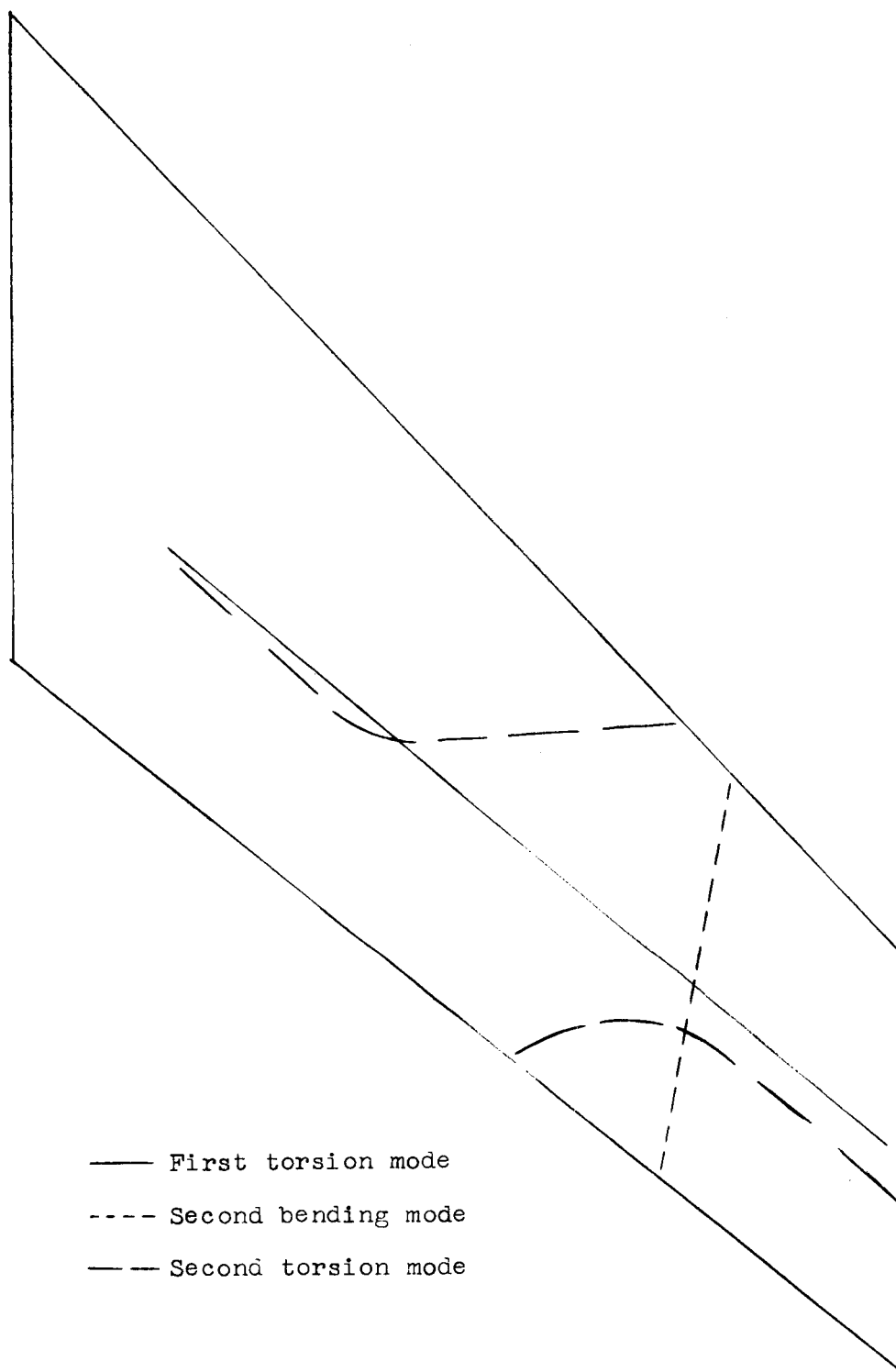


Figure 6.- Representative node-line pattern for semispan models.

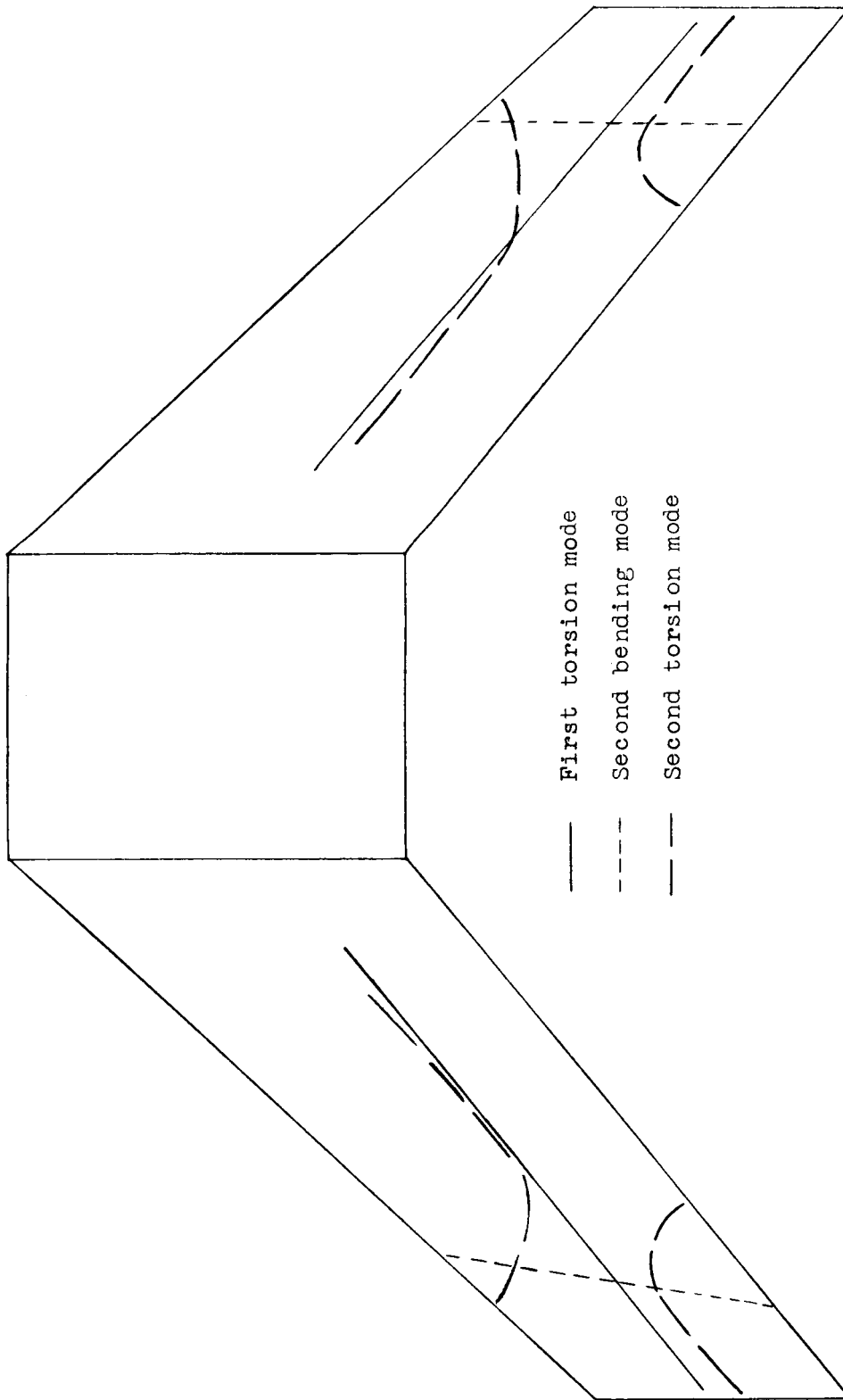


Figure 7.- Node-line pattern for full-span model.

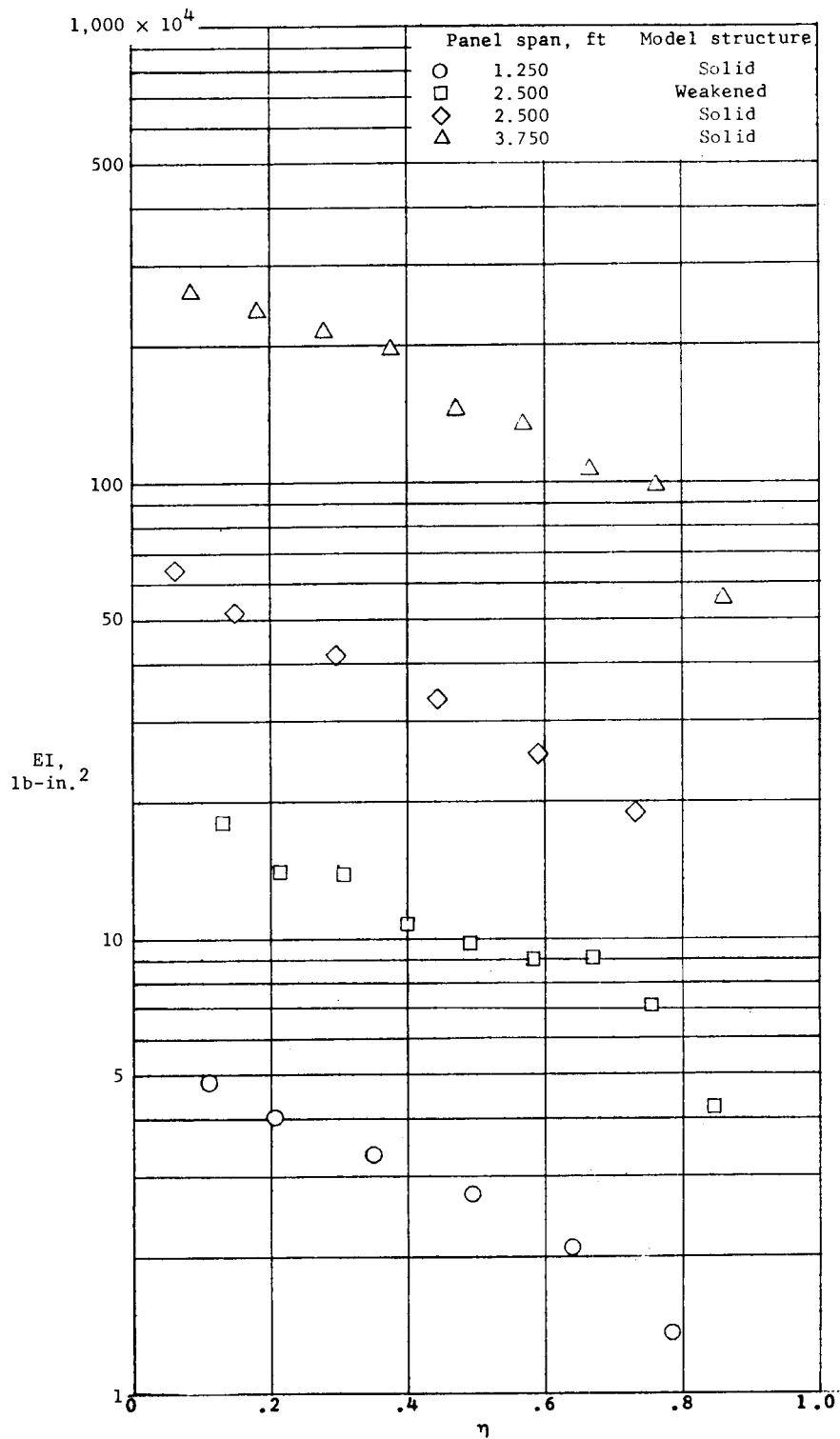


Figure 8.- Measured distribution of bending stiffness for representative semispan models.

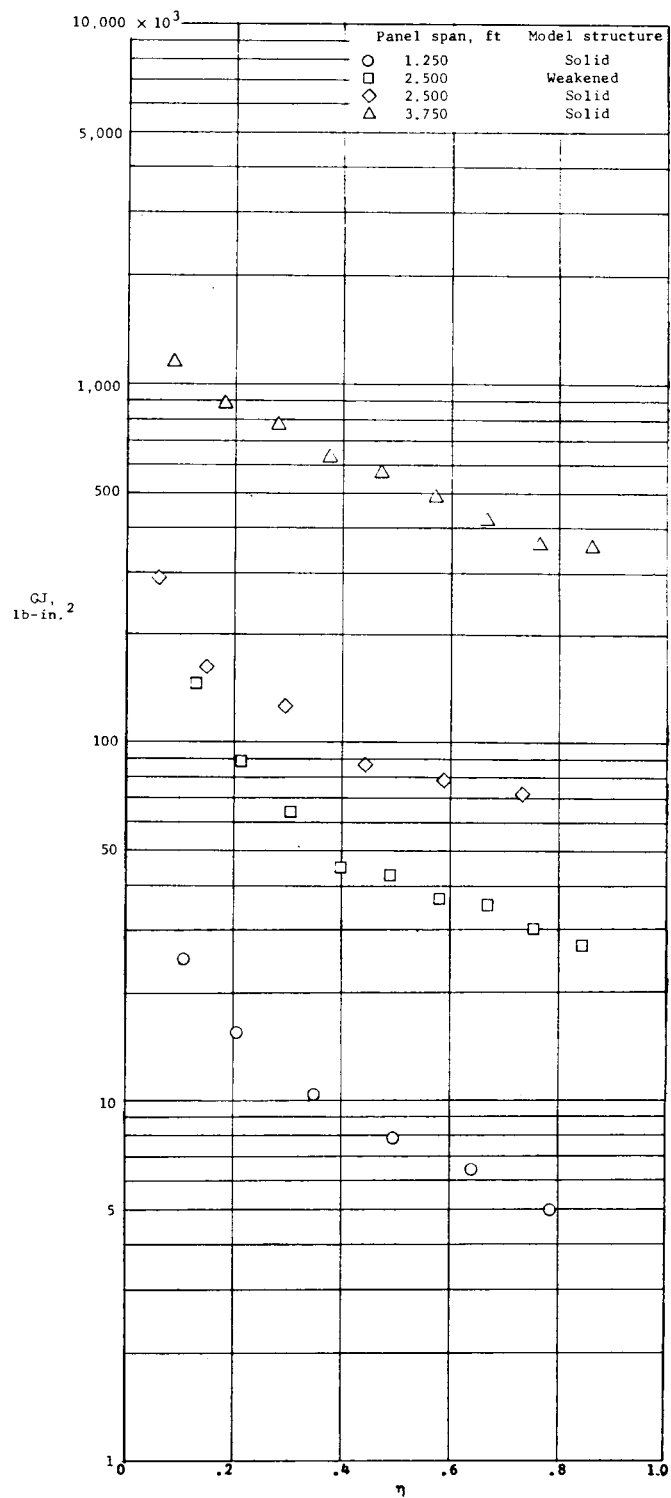


Figure 9.- Measured distribution of torsional stiffness for representative semispan models.

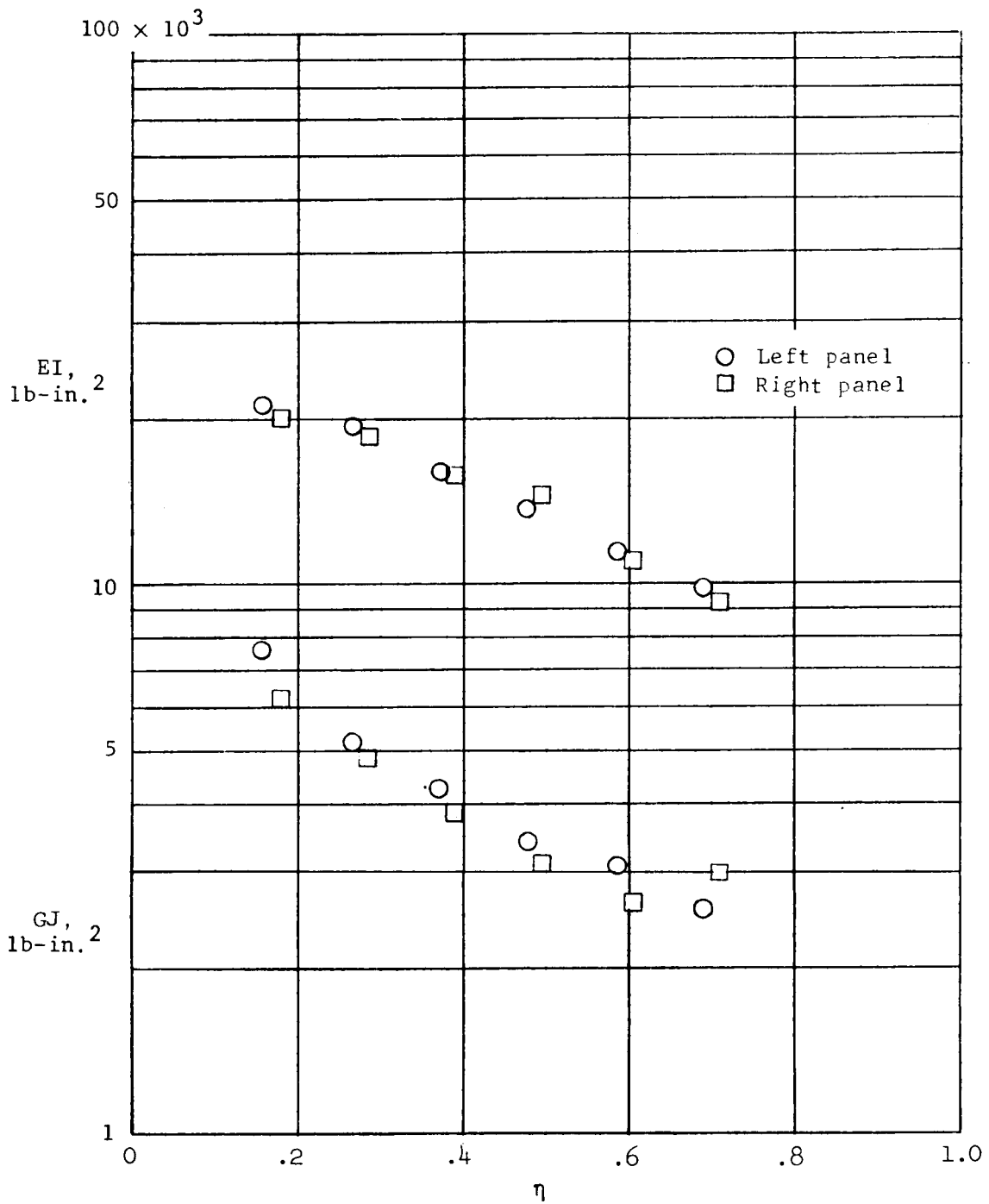


Figure 10.- Measured distributions of bending and torsional stiffness for the full-span model.

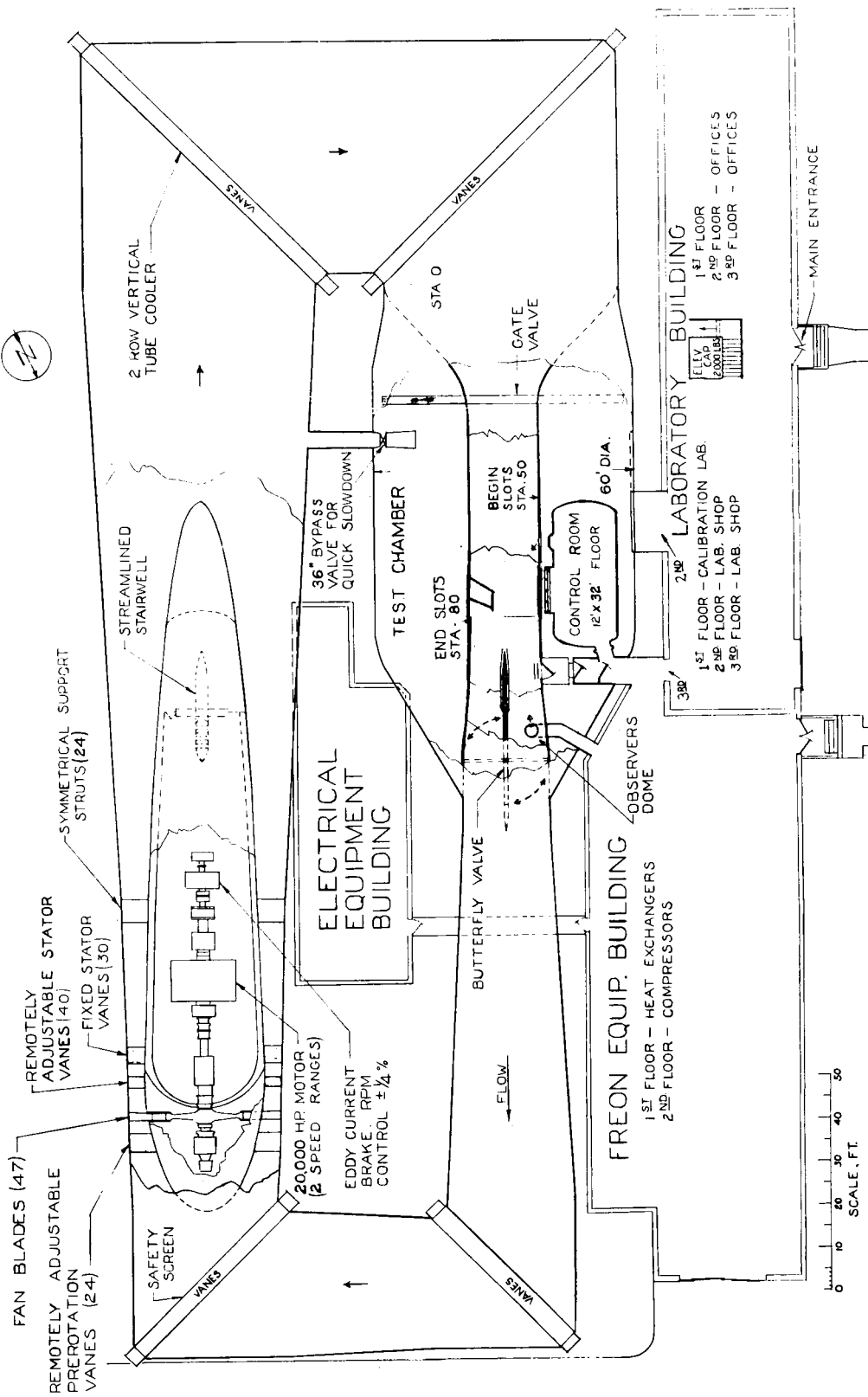


Figure 11.- General arrangement of the Langley transonic dynamics tunnel.

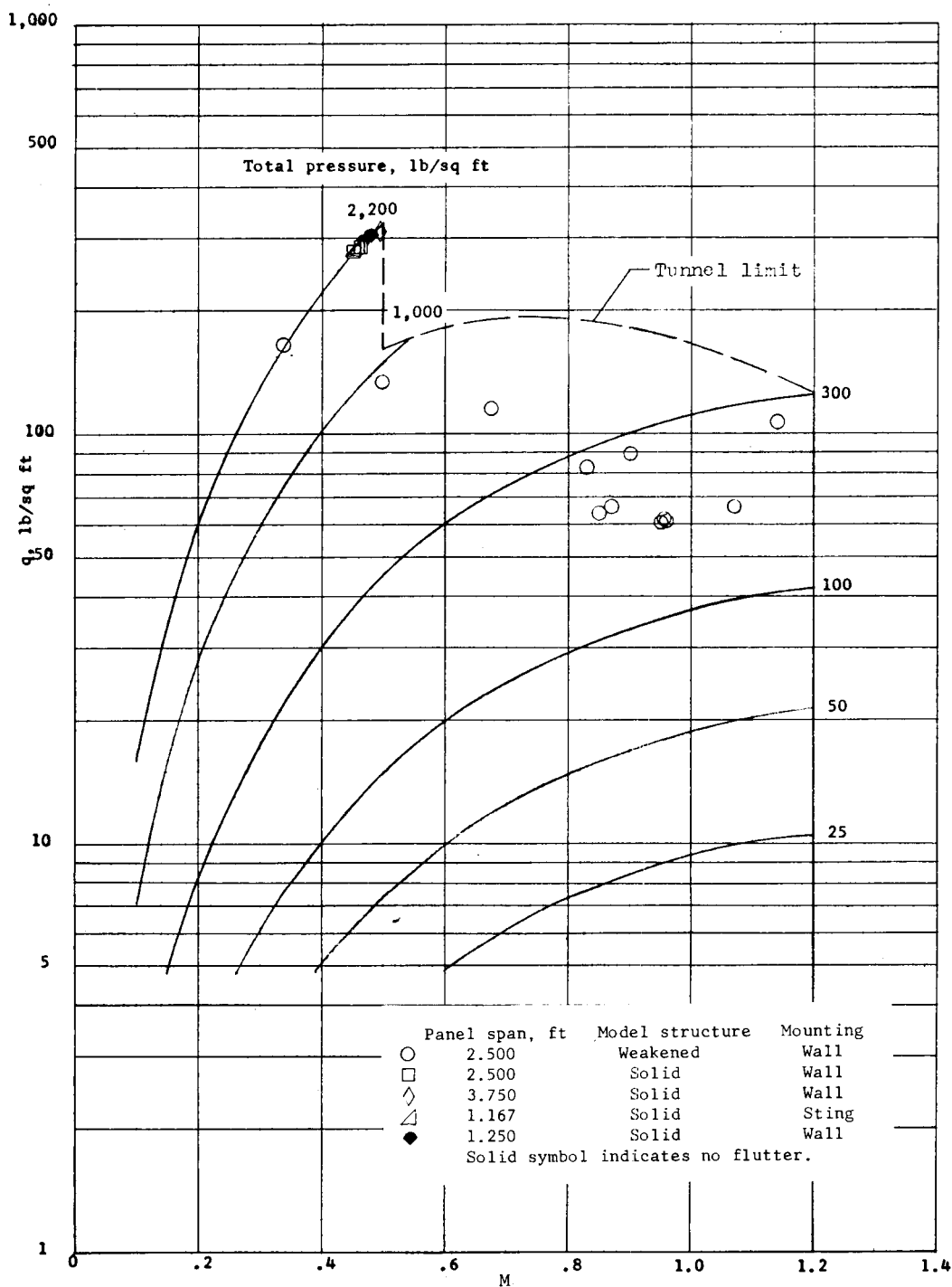


Figure 12.- Operating range of dynamic pressure, total pressure, and Mach number for air in transonic dynamics tunnel. (Symbols indicate flutter test points.)

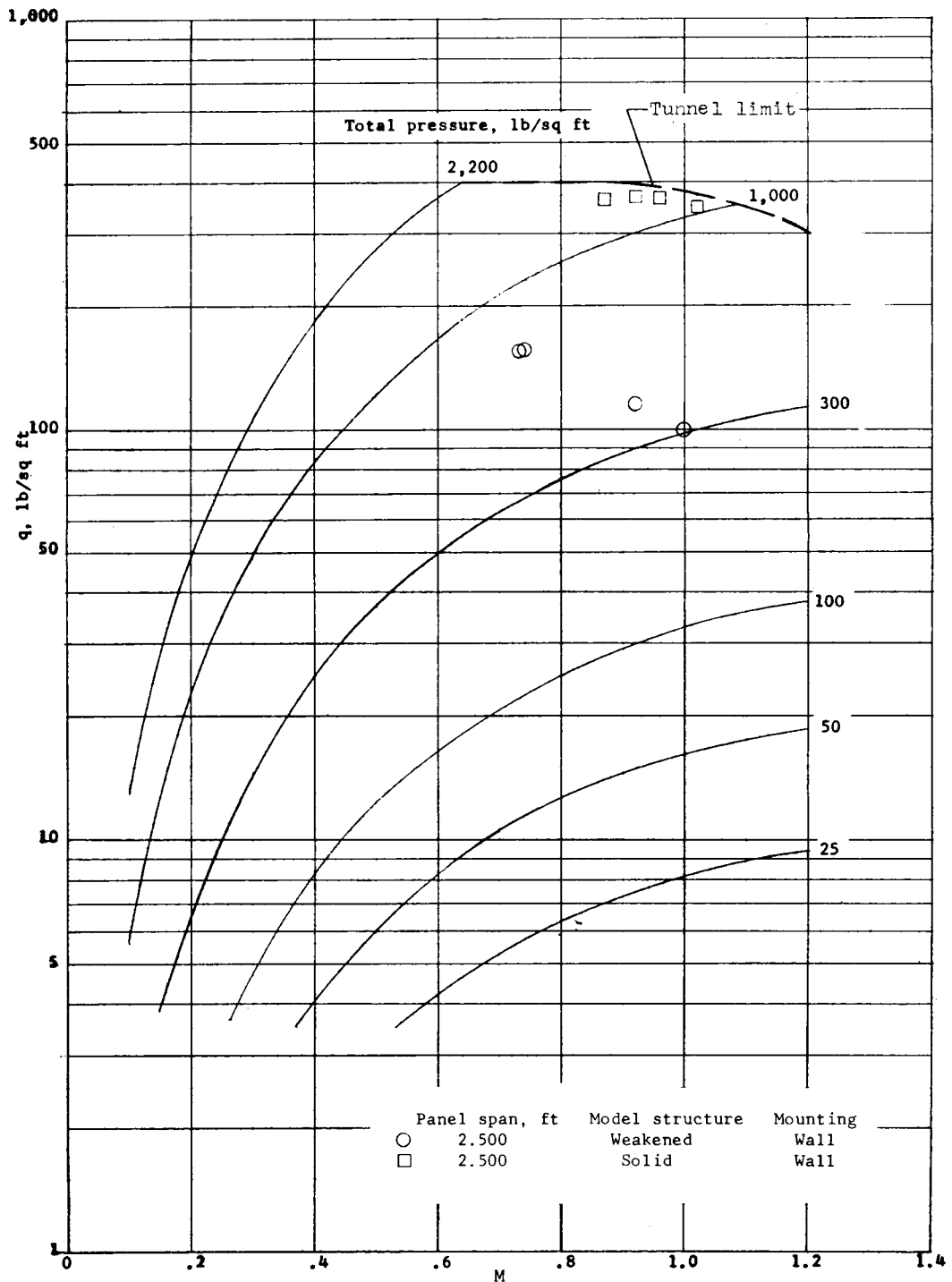


Figure 13.- Operating range of dynamic pressure, total pressure, and Mach number for Freon-12 in transonic dynamics tunnel. (Symbols indicate flutter test points.)

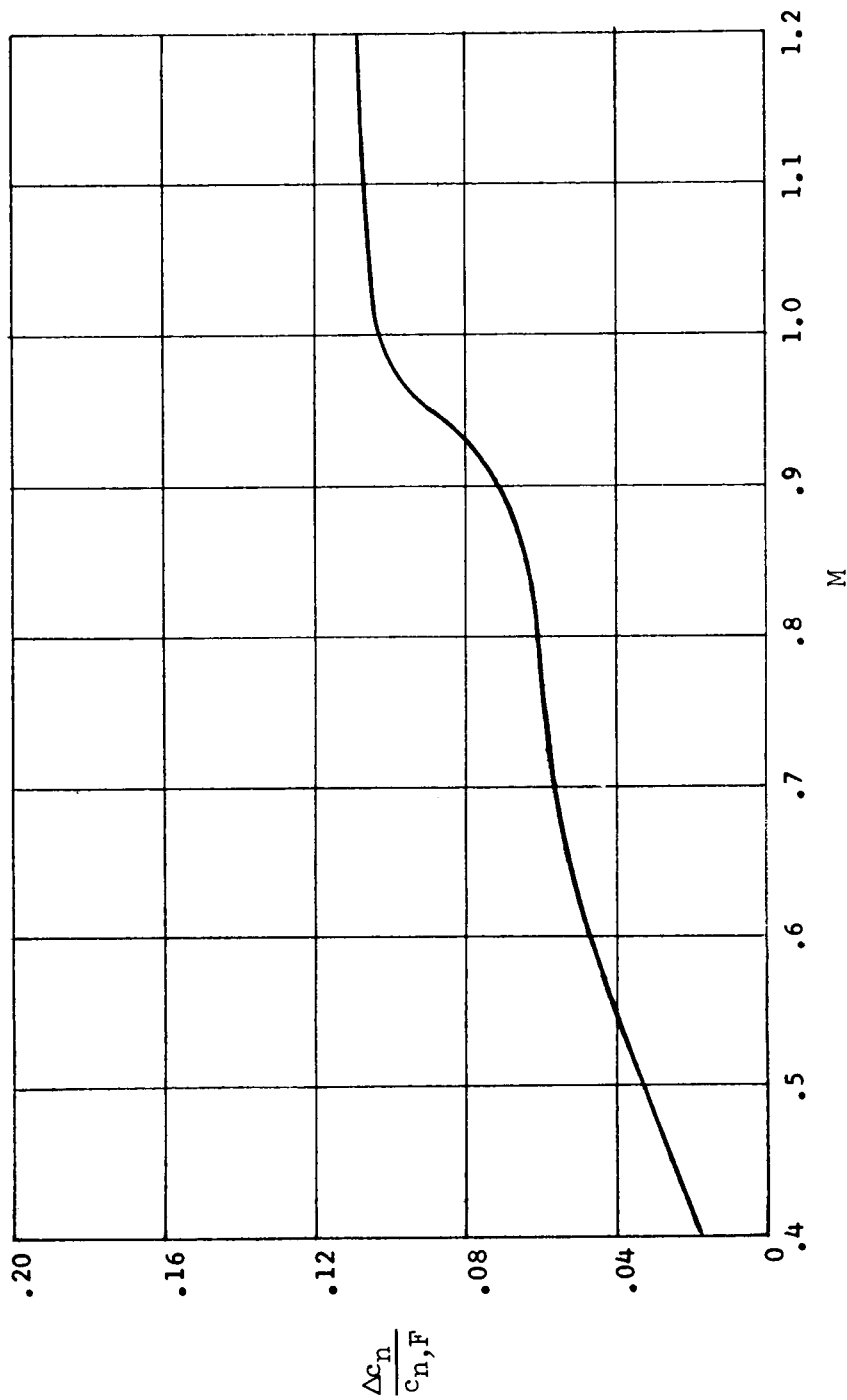


Figure 14.- Effect of Mach number on the difference between two-dimensional normal-force coefficient measured in Freon-12 and in air. Curve from figure 16 of reference 2.

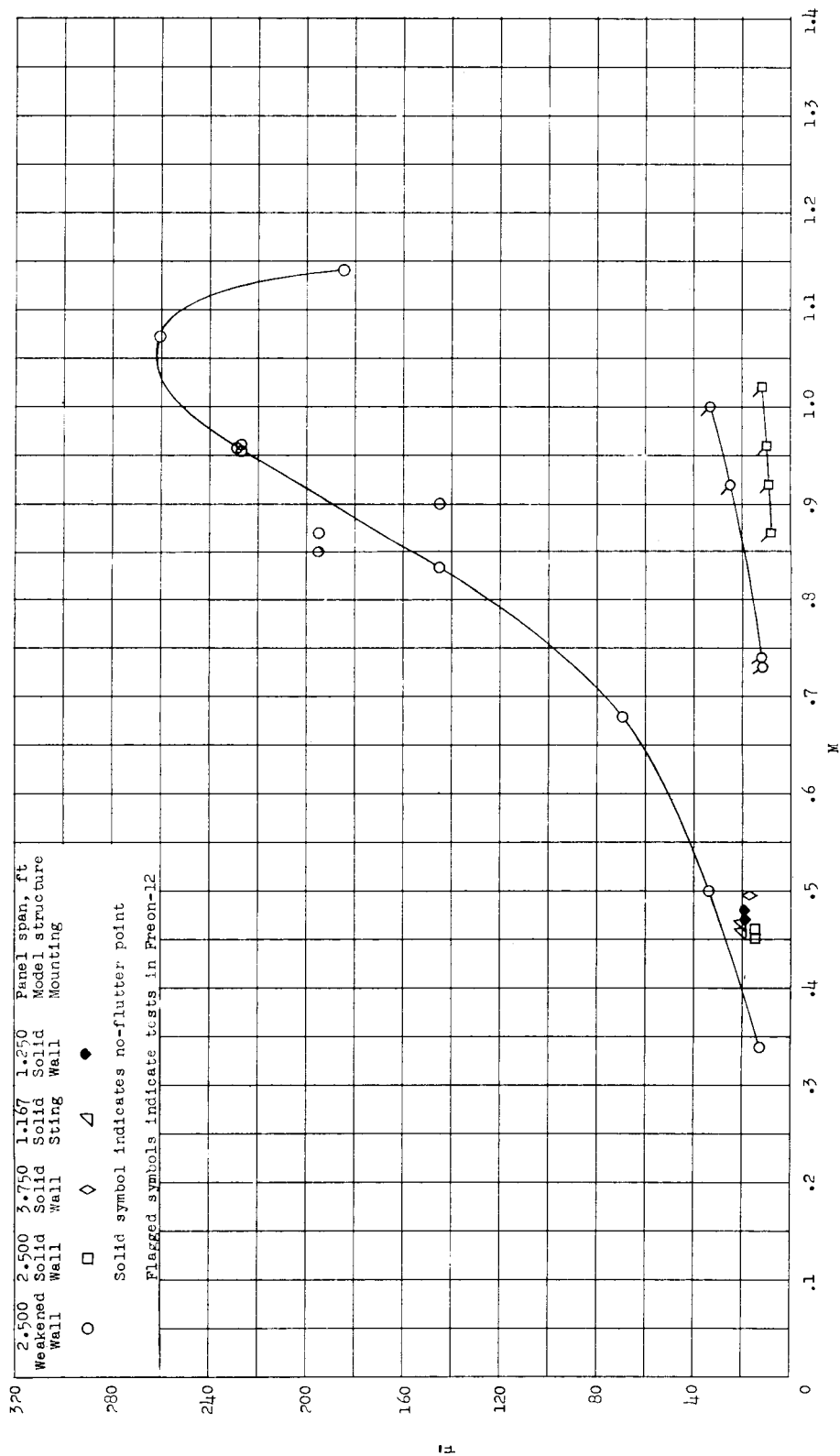
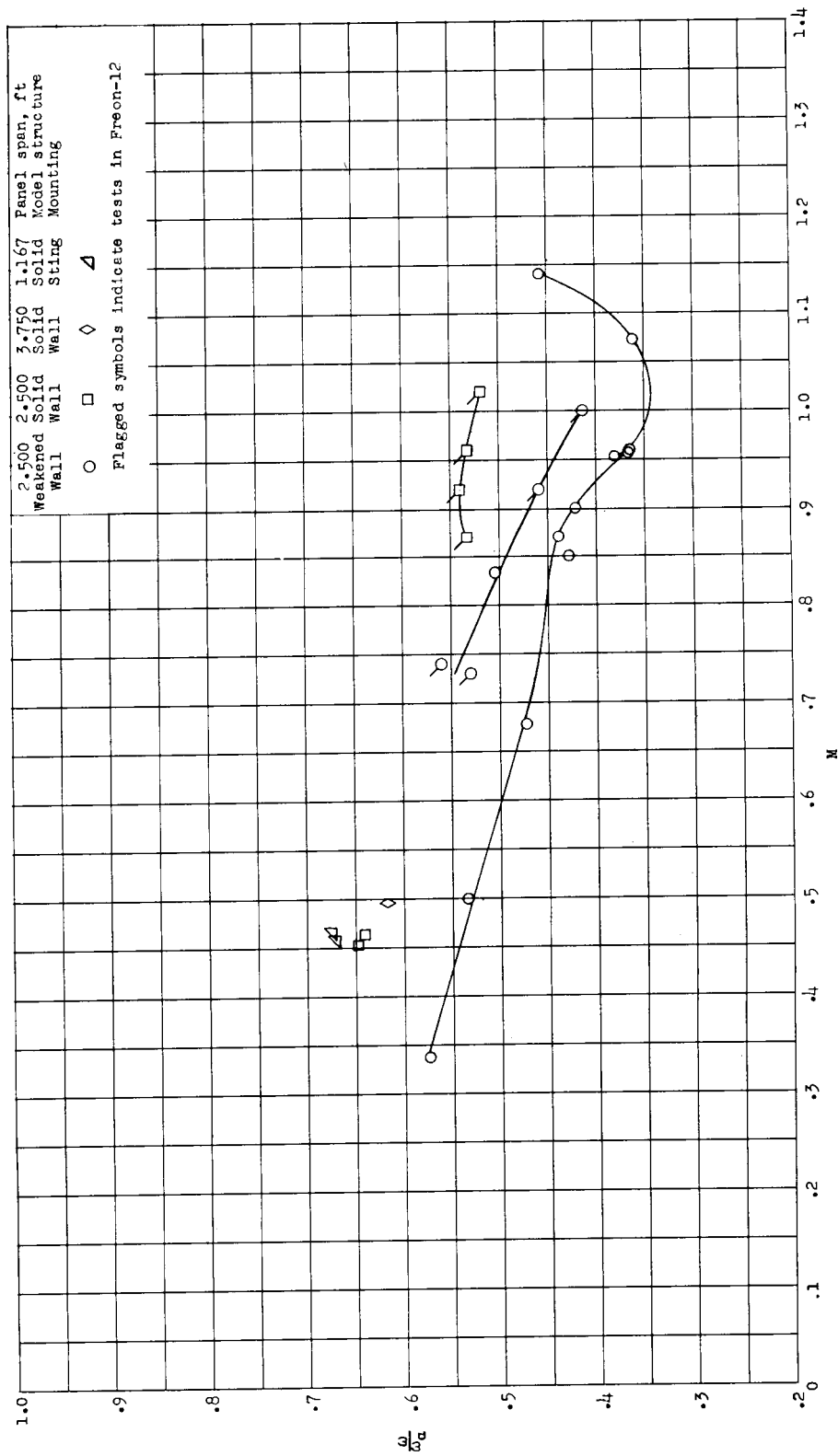
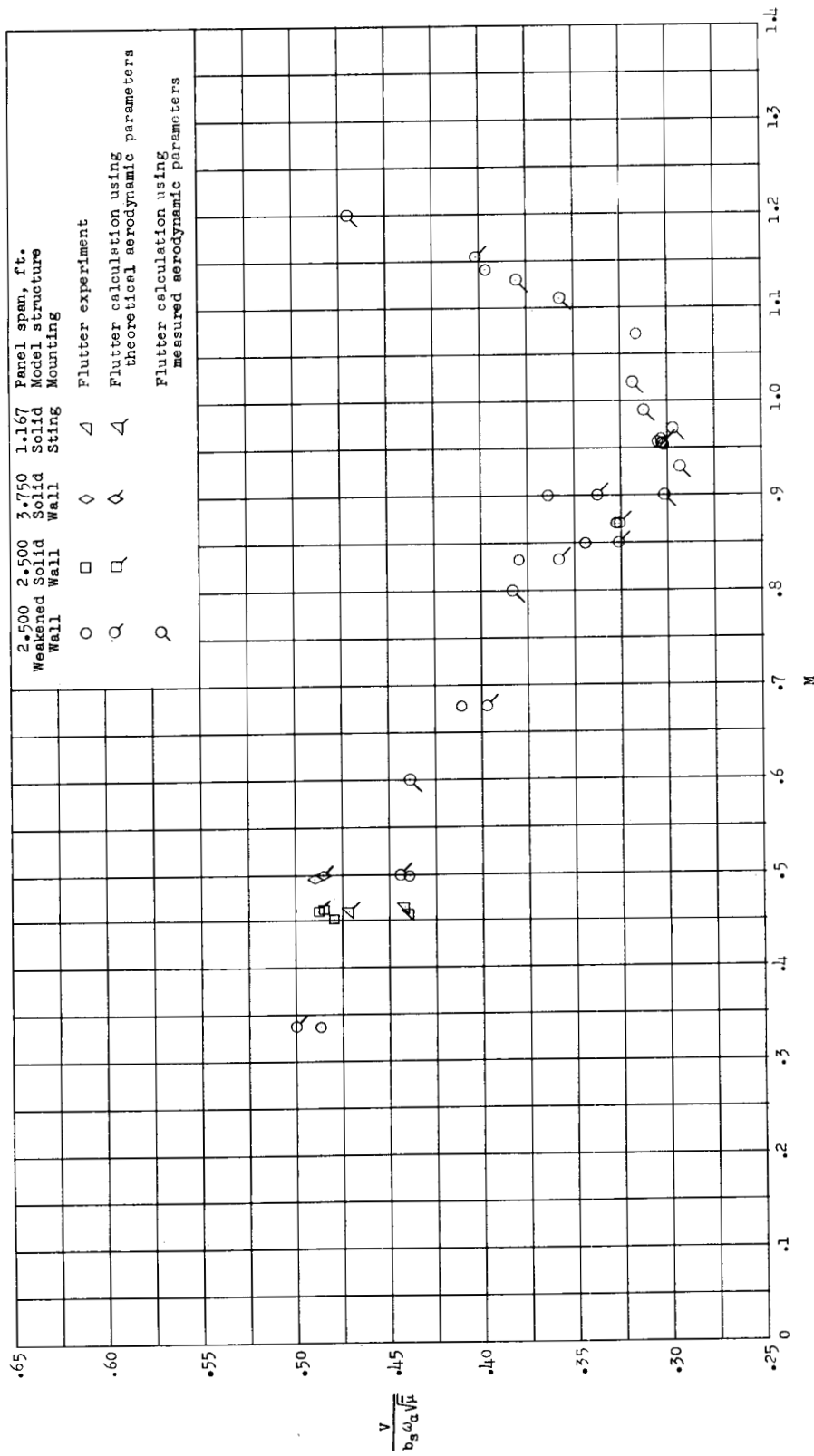


Figure 15.- Mass ratios and Mach numbers covered in the present tests in air and Freon-12 in the transonic dynamics tunnel.



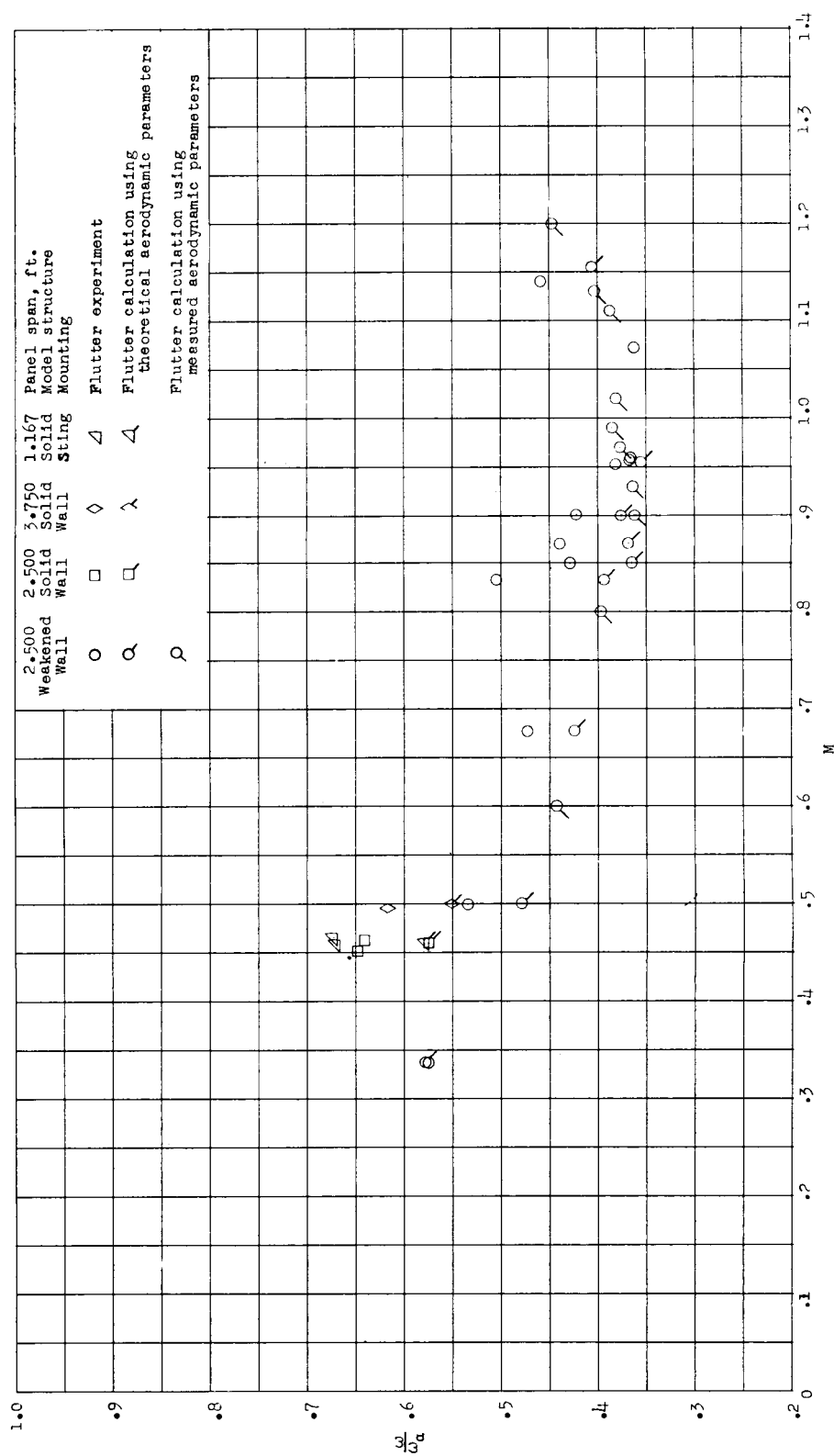
(b) Flutter-frequency ratio.

Figure 16.- Concluded.



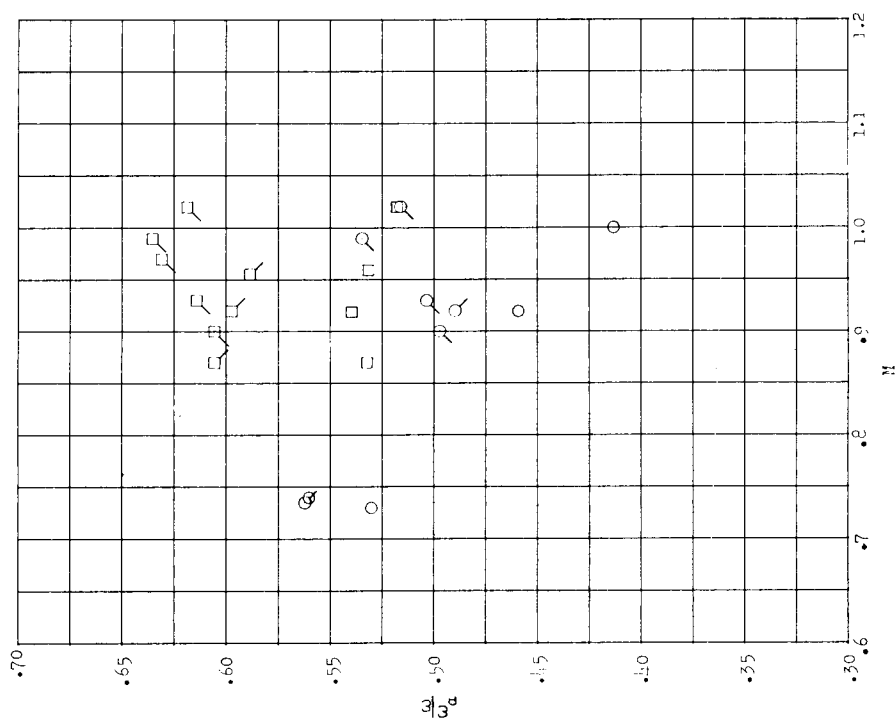
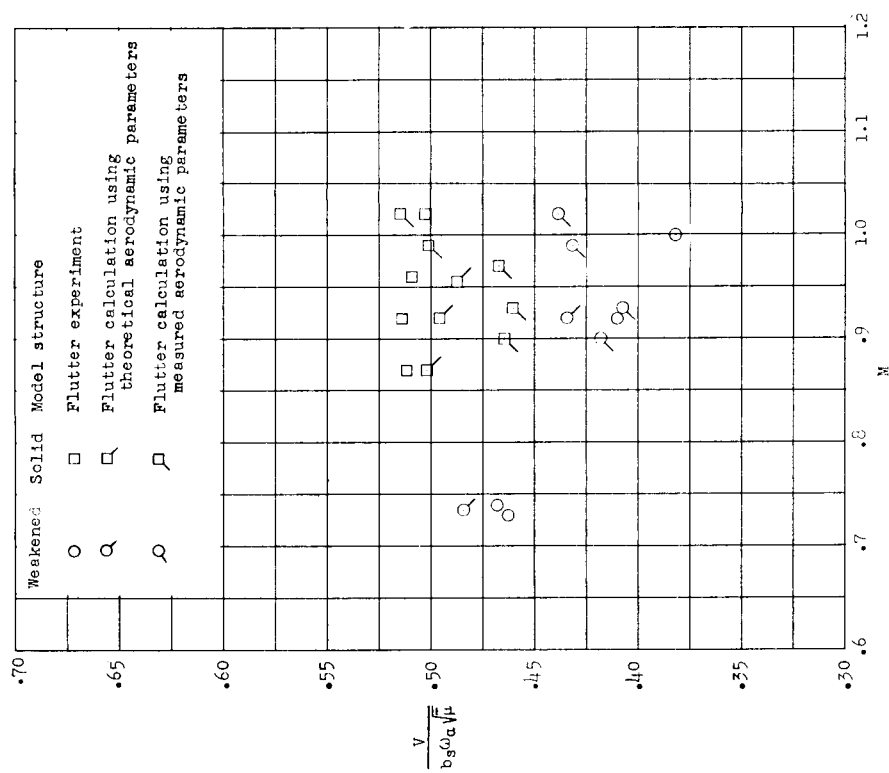
(a) Flutter-speed coefficient.

Figure 17.- Measured and calculated flutter characteristics for wings in air.



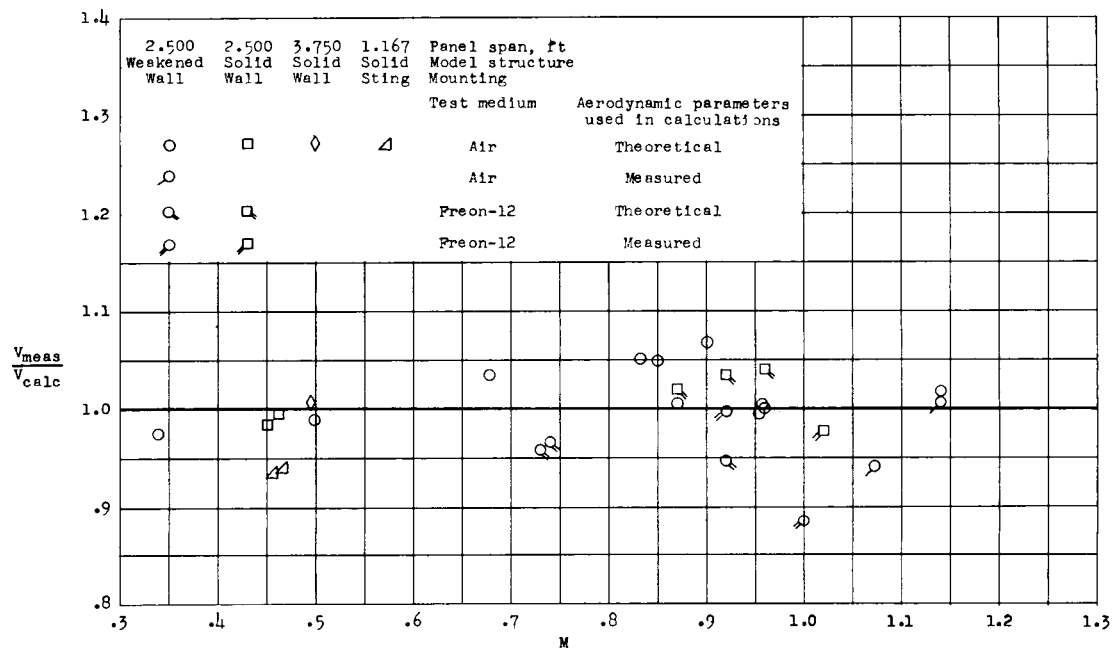
(b) Flutter-frequency ratio.

Figure 17.- Concluded.

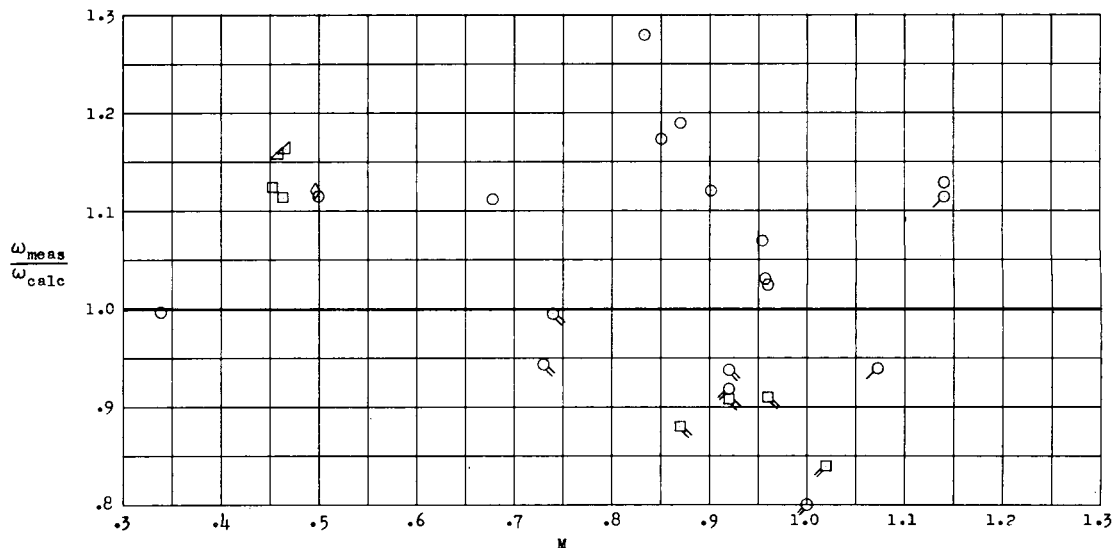


(a) Flutter-speed coefficient. (b) Flutter-frequency ratio.

Figure 18.- Measured and calculated flutter characteristics for 2,500-foot wall-mounted wings in Freon-12.



(a) Flutter speeds.



(b) Flutter frequencies.

Figure 19.- Correlation of measured and calculated flutter characteristics for wings in air and in Freon-12.

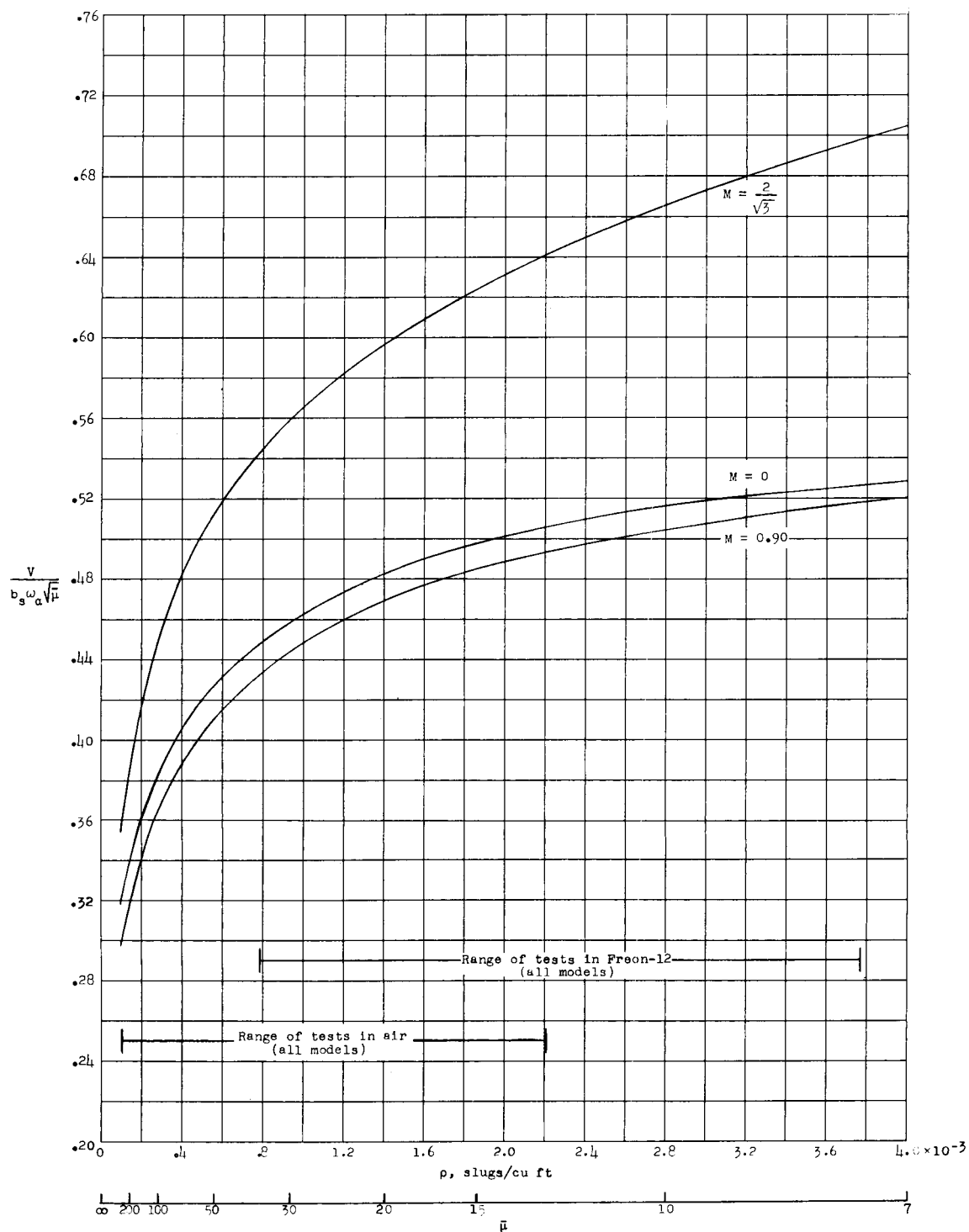


Figure 20.- Effect of density on the flutter-speed coefficients calculated for weakened 2.500-foot wall-mounted wings in air.

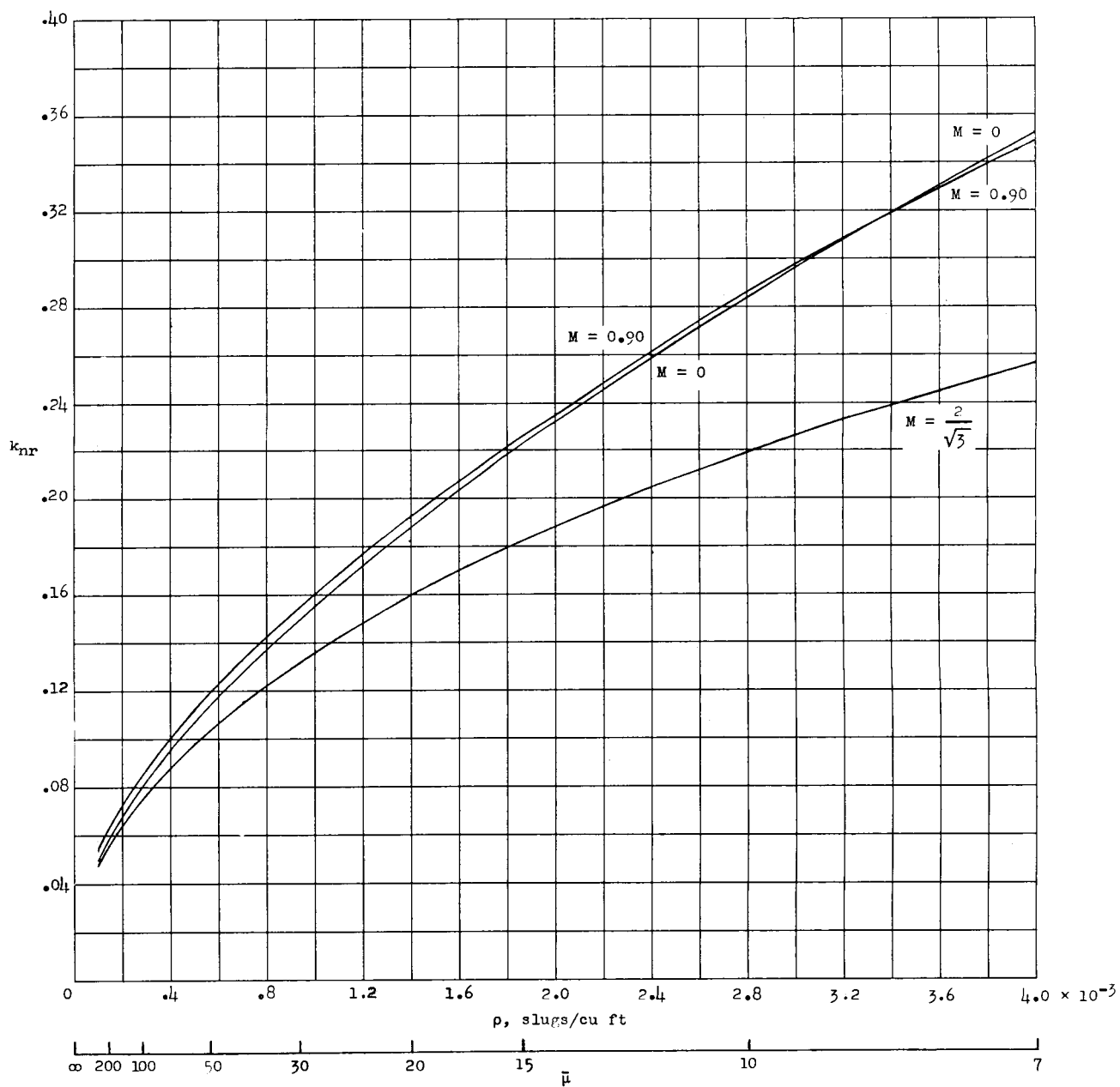


Figure 21.- Effect of density (or mass ratio) on the flutter reduced frequency calculated for weakened 2,500-foot wall-mounted wings in air.

